AFML-TR-72-46

IMPROVEMENT OF
TITANIUM ALLOY INGOT CONSOLIDATION

F.W. Wood
and
R.L. Carpenter
U.S. Bureau of Mines
Albany Metallurgy Research Center

Technical Report AFML-TR-72-46

May 1972

PRIOR REPORT LIMITED

Approved for public release; distribution unlimited.

Air Force Materials Laboratory
Air Force Systems Command
Wright-Patterson Air Force Base, Ohio

NOTICES

DOCUMENT CONTROL DATA - R & D

(Security classification of title, body of abstract and indexing annotation must be entered when the overall report is classified)

1. ORIGINATING ACTIVITY *(Corporate author)*	2a. REPORT SECURITY CLASSIFICATION
Albany Metallurgy Research Center U. S. Bureau of Mines P. O. Box 70, Albany, Oregon 97321	Unclassified
	2b. GROUP N/A

3. REPORT TITLE

Improvement of Titanium Alloy Ingot Consolidation

4. DESCRIPTIVE NOTES *(Type of report and inclusive dates)*

Final Technical Report   May 1970 - November 1971

5. AUTHOR(S) *(First name, middle initial, last name)*

Floyd W. Wood and Raymond L. Carpenter

6. REPORT DATE	7a. TOTAL NO. OF PAGES	7b. NO. OF REFS
May 1972	93	7
8a. CONTRACT OR GRANT NO. F 33615-69-M-5010	9a. ORIGINATOR'S REPORT NUMBER(S) AFML-TR-72-46	
b. PROJECT NO. 161-8A		
c.	9b. OTHER REPORT NO(S) *(Any other numbers that may be assigned this report)* None	
d.		

10. DISTRIBUTION STATEMENT

Approved for public release; distribution unlimited.

11. SUPPLEMENTARY NOTES	12. SPONSORING MILITARY ACTIVITY
	Air Force Materials Laboratory Manufacturing Technology Division (LTP) Wright Patterson AFB, Ohio 45433

13. ABSTRACT

An attempt was made to develop a manufacturing method for the elimination of nitride inclusions from titanium alloys as they are melted. The trial scheme involved skull casting as the first of two melting stages. Ten-inch-diameter ingots of Ti-6Al-4V were produced with artificial nitride defects added. The ingots were converted to one-inch-thick plates for evaluation. Preliminary results of examining rolled plates revealed that the proposed manufacturing method failed to eliminate the synthetic nitride-induced flaws. Also, the degree to which it may have helped is uncertain because of the appearance of extraneous types of defects and difficulties in finding and identifying defects. Metallographic specimens were prepared from all major defect areas. The defects were differentiated according to microstructure and their composition was determined by microprobe analyses.

1a

DD FORM 1473   REPLACES DD FORM 1473, 1 JAN 64, WHICH IS
NOV 65   OBSOLETE FOR ARMY USE.

14 KEY WORDS	LINK A		LINK B		LINK C	
	ROLE	WT	ROLE	WT	ROLE	WT
Metallurgy						
Nitride						
Ingot/Billet flaws						
Titanium						
Titanium alloys						
Melting						
Solidification						
Casting						

15

IMPROVEMENT OF

TITANIUM ALLOY INGOT CONSOLIDATION

F.W. Wood and R.L. Carpenter

/ C

FOREWORD

This Technical Report covers work performed under Contract F 33615-69-M-5010 from 1 May 1970 to 30 November 1971. The information was released by the authors on 1 April 1972 for publication.

This contract with the Albany Metallurgy Research Center of the Bureau of Mines, Albany, Oregon, was initiated under Manufacturing Methods Project 161-8A, "Titanium Alloy Ingot Consolidation Practice Suitable for Commercial Application." The project was administered under the technical direction of R.L. Kennard, Materials Processing Branch (LTP), Wright-Patterson Air Force Base, Ohio. Floyd W. Wood of the Bureau of Mines, Albany Metallurgy Research Center, was the principal investigator.

This project has been accomplished as a part of the Air Force Manufacturing Methods program, the primary object of which is to establish, on a timely basis, manufacturing processes, techniques, and equipment for use in economical production of USAF materials and components. The program encompasses the following technical areas:

Metallurgy   - Rolling, Forging, Extruding, Drawing, Casting, Powder Metallurgy, Composites

Chemical   - Propellants, Plastics, Textile Fibers, Graphite, Fluids and Lubricants, Elastomers, Ceramics

Electronic   - Solid State, Materials and Special Techniques, Thermionics

Fabrication   - Forming, Material Removal, Joining, Components

Suggestions concerning additional Manufacturing Methods development required on this or other subjects will be appreciated.

ii

This technical report has been reviewed and is approved.
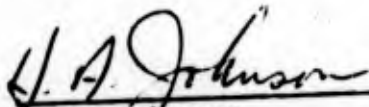
H.A. Johnson
Chief, Materials Processing Branch
Manufacturing Technology Division

ABSTRACT

An attempt was made to develop a manufacturing method for the elimination of nitride inclusions from titanium alloys as they are melted. The trial scheme involved skull casting as the first of two melting stages. Ten-inch-diameter ingots of Ti-6Al-4V were produced with artificial nitride defects added. The ingots were converted to one-inch-thick plates for evaluation. Preliminary results of examining rolled plates revealed that the proposed manufacturing method failed to eliminate the synthetic nitride-induced flaws. Also, the degree to which it may have helped is uncertain because of the appearance of extraneous types of defects and difficulties in finding and identifying defects. Metallographic specimens were prepared from all major defect areas. The defects were differentiated according to microstructure and their composition was determined by microprobe analyses.

Preceding page blank

TABLE OF CONTENTS

Preceding page blank

LIST OF ILLUSTRATIONS

LIST OF ILLUSTRATIONS (Continued)

LIST OF ILLUSTRATIONS   (Continued)

LIST OF ILLUSTRATIONS   (Continued)

LIST OF TABLES

LIST OF TABLES (Continued)

IMPROVEMENT OF
TITANIUM ALLOY INGOT CONSOLIDATION

1. INTRODUCTION

1.1 Background

An earlier contract, F 33615-68-M-5002, was reported by the Bureau of Mines (AMRC) in April 1969. (7)[1] Other related information was developed at TRW Inc. under Contracts F 33615-67-C-1737 and F 33615-69-C-1443, and reported in September 1968 (2) and May 1971 (3). These projects, including the current one, concern alpha-stabilized defects in Ti-6Al-4V.

In the Bureau of Mines work, it was decided that alpha-stabilized defects were predominately, but not exclusively, of an inclusion type. Then, on the basis of refractoriness, likelihood of occurrence, alpha-stabilizing capability, and micro-analyses of naturally occurring defects from commercial billets, it was concluded that most inclusions are nitrogen-rich. Therefore, a technique was developed for synthesizing alpha-stabilized defects by adding Ti_xN seeds (where $3 > x > 1.5$) to ingots as they were melted.

Three types of defects were found in the nitride-seeded metal. There were friable, hard and incoherent inclusions of delta- and/or epsilon-phase Ti-N materials surrounded by alpha-stabilized reaction zones. These were called Type I defects. They usually generated some sort

---

[1]Underlined numbers in parentheses are references.

of a void when the metal was deformed. Type II defects were hard, coherent lumps of alpha-phase material with microstructures resembling the alpha-stabilized reaction zones associated with the Type I defects. Deformation sometimes caused small voids or cracks at Type II sites, but usually this did not happen. Type III defects were localized dispersions of apparently coherent microinclusions in one to several contiguous grains. They seemed to cause no problems during deformation. An electron microprobe was used for compositional microanalyses of defect regions, and nitrogen richness was found only in Type I defects. In the Type II and Type III regions nitrogen was below the detection limit (~1.5% at that time), and it was only apparent that the "average" atomic number at these sites was less than for the bulk matrix. It was presumed on the basis of circumstances, that the Type II and III defects were caused by nitride seeding, but direct evidence of this was not obtained. In all cases, alloy segregation was detected in alpha-stabilized regions. The V content was especially affected. It became concentrated in β-phase material and depleted in α-phase material.

In a third part of the investigation, melting practices were varied for 4- and 5-inch-diameter ingots and the effect of the variations on the survival of nitride defects was studied. In cold-mold arc melting, factors that tended to alleviate ingot defectiveness were good vacuum, high arc current, melting more than once, and pneumatic vibration of melts. Unidirectional magnetic stirring and electroslag melting seemed to have no advantages and may have been disadvantageous with regard to nitride inclusions. Overall, the best results were obtained by skull casting. In fact, two 4-inch-diameter skull castings appeared to be free of nitride inclusions.

The present project was conceived as a means of testing and exploiting the earlier encouraging results by attempting to develop an improved manufacturing technology utilizing skull casting as one stage of melting. The work was done on a scale leading to 10-inch-diameter remelt ingots.

2

2. INVESTIGATION

2.1 Basic Equipment, Procedures, and Materials

The trial process started with pressed sponge bars of Ti (2"x2"x10"), containing alloy and nitride seeds. The sponge was magnesium-reduced, vacuum-distilled material from the GSA stockpile. One sample apparently contained anomalously high amounts of Al and Mn, but the only consistently high contaminant was carbon at about 500 ppm. The hardness of as-cast buttons was about Bhn 125. More detailed results of sponge analyses are given in tables I, II, and III. Initially, alloy was added as a combination of a 15Al/85V master alloy plus elemental Al. This material went into the first 10" remelt (SA 26,869) and part of another (SA 26,956). Thereafter, a 60Al/40V master alloy was used. (See tables IV and V for master alloy analyses.) In all cases, the alloy was distributed along the bar. The inclusion seeds consisted of broken pieces of nitride (TiN) that had been prefused with a W-electrode arc. The nitrogen content of this material was typically in the range of 10 to 15 weight percent. About 1 g was placed near the center of each 2.5 kg sponge bar. Groups of 12 bars, or equal, were joined by W-arc welding in an inert-gas glove box to obtain electrodes for skull casting. The distribution of nitride seeds in electrodes incidentally imposed an extra severe test on the skull-casting process. Because electrode sections were ten inches long, there was always a pocket of nitride within about five inches of the end of an electrode. Thus there were never more than five inches of electrode left to be consumed when the last nitride seeds were added to the molten pool in the casting ladle. This meant that some nitride lumps always spent relatively little time in the pool and had a chance of still being near the surface when the pour was made. Near the end of the program, some massive casting scrap that contained nitride inclusions was recycled by substituting it for some of the pressed bars in sponge electrodes.

3

TABLE I. - Spectrographic impurity analyses, GSA sponge Ti, Purchase Order P-391466, 4/30/69

Element	Sample 1 A	Sample 1 B	Sample 2 A	Sample 2 B	Sample 3 A	Sample 3 B	Sample 4 A	Sample 4 B	Sample 5 A	Sample 5 B
Na	low	low	low	low	low	low	low	low	low	low
Mg	80	80	40	40	80	80	80	80	80	80
Al	40	3,000	300	30	300	100	100	100	100	100
Si	<30	90	<30	<30	<30	<30	<30	<30	<30	30
Ca	<10	<10	<10	<10	<10	<10	<10	<10	<10	<10
V	<40	<40	<40	<40	<40	<40	<40	<40	<40	<40
Cr	<10	<10	<10	<10	<10	<10	<10	<10	<10	<10
Mn	<50	1,000	500	<50	200	<50	<50	300	<50	200
Fe	<10	50	<10	10	10	300	20	<10	80	30
Ni	<20	<20	<20	<20	<20	<20	<20	<20	<20	<20
Cu	20	20	<10	300	10	10	10	10	10	10
Mo	<15	<15	<15	<15	<15	<15	<15	<15	<15	<15
Sn	<100	200	<100	<100	<100	200	<100	<100	100	<100
Pb	<100	<100	<100	<100	<100	<100	<100	<100	<100	<100

NOTE: All values in ppm.
Chlorine content is about 160 ppm as determined by separate chemical analysis.

4

TABLE II. - Analyses of buttons from GSA sponge Ti, Purchase Order P-3991466, 4/30/69

Element	Sample 1	Sample 2	Sample 3	Sample 4	Sample 5
N	140	135	129	121	143
O	952		447		747
H	37		50		48
C		541		492	

TABLE III. - Hardnesses of buttons from GSA sponge Ti, Purchase Order P-3991466, 4/30/69

Sample no.	As-cast, R_A	Machined surface, R_A	Ground surface, Bhn
1	45	48	131, 128
2	47	48	146, 140
3	49	53	170, 168, 163
4	43	48	146, 142, 143
5	47	50	152, 146, 152

NOTE: Rockwell values are averages of 3 to 5 determinations. In steel, the Brinell equivalents of the as-cast R_A values would be 117, 127, 136, 108, and 127, respectively. Machined surfaces may have been work hardened and specimens may have been too thin for accurate Brinell indentations.

TABLE IV. - Analyses of Al-V master alloy, Purchase Order P-3900028, 7/8/69

Al	V	Si	O	C	H	N
56.6%	41.7%	2,500	700	900	34	120

NOTE: All values in ppm except as noted.

TABLE V. - Analyses of Al-V master alloy, on hand from previous purchase

Al	V	B	Cr	Cu	Fe	Mg	Mn	Mo	Si
13.9%	82.7%	<100	<300	<30	<1%	<10	<3,000	<1%	<3%

NOTE: All values in ppm except as noted.

The 4-inch-diameter castings produced under the earlier contract were remelts. That is, the skull-casting operation was the second stage of melting. However, in the present program, it was decided to reverse the order and use skull casting as the first melting step. There were two main reasons for this: there is little opportunity to hot top a skull casting, and skull-cast ingots are generally limited to smaller sizes than are common for commercial CEVAR products. Regardless of the reasons, the decision may have influenced the overall results significantly.

For remelting into a 10" crucible, 7- to 8-inch-diameter first melts were desired, but the capacity of the casting ladle available was sufficient to fill an 8-inch cylinder only about 4-inches tall. It happened that the first melt electrodes were large enough (about 30 kg) to fill the ladle twice. Therefore a double pouring procedure was adopted. Two pours were made, in succession, into the same mold. Molds were made of machined graphite, and a 1.5-inch-diameter stud was integrally cast at the bottom center of each ingot. At first, the studs were cast with threads, but later they were cast plain and the threads were machined in afterwards. The top of each ingot was drilled and tapped with a matching hole, and both end faces were sampled and flattened by machining. Selected groups of the ingots were then screwed together, each in an inverted position (stud up), to form electrodes for remelting. The use of integrally cast studs avoided introducing extraneous metal in the form of threaded couplings. The direct current arc for skull casting was typically operated at about 5,800 to 6,000 amperes and 30 to 32 volts, straight polarity. The furnace was dynamically pumped by a 1,250-CFM lobe-type blower.

The remelting furnace was a straightforward CEVAR unit, equipped with a 110-CFM rotary piston mechanical pump. During most of each melting cycle, the arc was operated at 7,500 to 8,000 amperes, 30 to 32 volts, straight polarity.

7

At the end of each cycle, an on-off hot-topping procedure was followed. This involved interrupting the arc, observing the ingot top surface through a remote viewing system, reigniting the arc just before the molten surface froze into the center, and extinguishing the arc again after some 15 to 45 seconds. The ingot surface was "blasted" two or three times at each of three successively lower power levels -- 5,000 to 5,500 amperes, near 4,000 amperes, and about 2,500 to 3,500 amperes. This practice was based on good results in past experience. Hot topping by decreasing power without interruption is precluded by the particular rectifier control system in use.

Remelted ingots were conditioned by machining them in a lathe. Ends were squared and sidewalls were scalped to remove traces of spatter, crust, and scale. Analytical samples were also collected at this time. The as-cast ingots were then inspected ultrasonically to locate the regions of shrinkage or gasiness near the ingot tops. An echo technique was used, and an oil film on the ingot surface served to couple 2.25 and 5.0 MHz transducers to the metal. In most cases, the defective region was removed by sawing, and the new top face was reconditioned by machining.

Ingots were first broken down to slabs, nominally 4" by 7" in cross section, by forging. Preheating was generally at 1,090°C for about 2 hours, and there were typically six reheatings at the same temperature, each for 30 minutes. Three forging passes were made after each heating. The 4" slabs were then air cooled and cut to more manageable lengths. Forging was then continued to obtain 2" by 7" slabs. The same sort of practice was followed, but with only two reheatings. Slabs were then air cooled and cut again. Finally, the slabs were heated to 850°C for rolling to 1" by 7" plate. The rolling was done in about 9 to 12 passes with one intermediate reheating for 30 minutes. The plates were air cooled, and oxide scale was removed by sand blasting.

There were four exceptions to the conversion practice just described. (1) The first ingot produced (SA 26,869) was actually forged at a temperature near 960°C because of a poorly calibrated temperature controller on the pre-heat furnace. In this particular case, surfaces of the 4"-thick slab were machined before the forging was completed. (2) The bottom half of the third ingot produced (SA 26,956) was rolled at 950°C instead of 850°C, but no advantage was noted, so 850°C was used thereafter. (3) Two ingots (SA 26,869 and SA 26,917) were forged without cropping the shrinkage region from the ingot tops. (4) Because of short lengths, two ingots (SA 26,917 and SA 27,172) were forged all the way to 2" slabs without cooling down and cutting at the 4" stage.

All plates were inspected ultrasonically. This service was provided by Wah Chang Albany Corporation. An immersion-type, C-scan, echo technique was used. Initially, test standardization was specified at 80 percent of saturation on a 20-mil flat-bottomed hole at a depth of one inch when a 5 MHz signal was used in Ti-6Al-4V. In practice, although 5 MHz sound was used, it became necessary to relax the sensitivity somewhat at operator discretion in order to cut out signal "noise" originating at or just below sand-blasted surfaces. In all cases, a 20-mil hole in a test block was still indicated on record charts, even though it may have been barely resolved. In one case (ingot SA 26,956) it was necessary to machine plate faces in order to complete the ultrasonic inspection at all. Better surface conditioning probably should have been practiced more generally. It might have avoided some problems of record interpretation, or at least eliminated a complicating factor. Inspection records were provided in the form of 1-to-1 strip charts.

In some cases, plate sections that appeared defective in ultrasonic tests were selected for X-ray radiography. This work was done by Albany Metallurgy Research Center personnel, using X-ray facilities of the Metallurgical

Engineering Department, Oregon State University. The X-ray source tube was operated at 120 kv, 5 ma. "No-screen" film was exposed for about 4.5 minutes behind the rolled plates at 36 inches from the source. Development in X-ray developer for 5 minutes at 70°F gave background densities in the range of 1.7 to 2.0.

Finally, on the basis of the nondestructive tests, an attempt was made to characterize selected flaws by destructive sectioning and metallography, including some microprobe examinations.

2.2 Program Implementation

Many of the procedural details given in the foregoing part of this report had to be established or verified in a series of preliminary tests. For example, defective sections of ingots left on hand from Contract F 33615-68-M-5002 were used in trials of the conversion and nondestructive testing practices. As a final test, the procedures were combined to produce, convert, and examine a 10-inch ingot (SA 26,869). The first melts for this ingot were skull cast by pouring directly into the open top of a split graphite cylinder. One of the castings (SA 26,837) produced this way was split lengthwise. Later a half-inch-thick slice was removed. The main reason for exposing the cross section of the casting was to inspect the integrity of the joint between the first and second incremental pours. However, the main result was the revelation of several small Type I and II defects in a narrow band just above the top of the first pour. This discouraging event caused some reconsideration and delay.

Electron-bombardment (EB) melting and inductoslag melting were considered as possible substitutes for skull casting in the first stage of melting, and some variations of skull-casting technique were tried. Results with inductoslag melting and consumable-electrode EB melting were

discouraging. Both methods seemed to have less effect on nitride inclusions than skull casting did.

Melting of buttons by electron bombardment may have been more successful, but the results were really inconclusive. Three 60 to 70-gram buttons of Ti-6Al-4V alloy were melted with implanted nitride seeds, but without in-process metal feed. Each button was melted on one side, turned and melted on the other side. The melting times were 10 minutes (5 min per side), 20 minutes (10 min per side), and 30 minutes (15 min per side). After some futile attempts to find residual nitride inclusions by random cutting, remaining material was rolled at 850°C to 40-mil sheet. It was expected that any nitride inclusions of significant size would cause bumps or cracks on the surfaces. Indeed, some flaws were found on the surfaces, especially on the sheet from buttons melted 10 and 20 minutes. Metal containing the defects was cut out and metallographically prepared. The specimens were examined optically and by electron microprobe. Optically, each specimen appeared to include some hard material. In general, the flaw size decreased for the longer melting times. In addition, it was only in the metal melted for 10 minutes that flaws had a reaction zone associated with them. An example is shown in Figure 1. With the microprobe, X-ray analysis indicated that a Ti-Al-V oxide was associated with all flaws, and only one specimen, from metal melted 10 minutes, contained some material with high nitrogen content (near 7%).

It is likely that the oxides were formed during hot rolling as the surface flaws opened up. However, the question of what happened to the nitride seeds is still unanswered. It is possible that small nitride inclusions caused the surface defects, but that the nitrides themselves were either lost or oxidized during the rolling. Even so, the size and number of the flaws indicates that most of the added nitride was either decomposed or dissolved. But this result is strictly conjecture, and

11

FIGURE 1. - Micrograph (originally 150X) of
inclusion EB-1

furthermore some separate experiments in this laboratory
have indicated that the stability of the Ti-6Al-4V alloy
is poor during electron-bombardment melting. After 10
minutes of melting the Al content was reduced to 2.44%,
and, after 20 minutes, it dropped to 0.65%. Short melt-
ing times would minimize alloy loss, but at the same time
the chance of dissolving refractories would be reduced.

The variations of skull casting tried were: first,
pouring onto a tundish and letting metal overflow into the
cylindrical mold; and second, pouring through a side-
gated funnel and sprue. Only the latter technique seemed
promising. The practice is illustrated in Figs. 2, 3, and
4. Figure 2 shows a filled mold before disassembly, ex-
cept that a cover plate is removed from the section at the
left. Figure 3 shows the casting with the mold almost all
removed, and Fig. 4 is a polished and etched cross section
of a similar casting (SA 26,931). The mold was designed
with a section of the sprue extending below the lower gate.
This served as a trap for the first metal poured. The first
half of each casting filled the mold just about to the
top of the lower gate. Thus another section of sprue,
between the two gates, served to trap the first part of
the second pour made into the mold. This trapping feature
was based on the observation, in direct-pour skull cast-
ings, that surviving inclusions were contained in some of
the first metal over the lip of the casting ladle. The
traps also caught spatter beads that were free to enter
the funnel during melting.

When the casting shown in Fig. 4 was cut up, no in-
clusions were discovered. However, several Type I and II
defects were found in the associated sprue, mainly at the
bottom of the upper trap section. With this reassurance,
the side-gated skull casting process was retained in com-
pleting the rest of the program.

Overall, eleven ten-inch ingots were produced. They
are listed in Table VI. Either seven or eight of the ingots

13

TABLE VI. - <u>Identification of ten-inch remelt ingots</u>

Ingot number	As-cast weight, kg	lb	Remarks
SA 26,869	119.7	263.9	electrode was direct-pour skull castings.
SA 26,917	64.6	142.4	third melt of 5" ingots produced for Contract F 33615-68-M-5002; original sponge was different than for other ingots listed here.
SA 26,956	131.5	290.0	electrode was side-gated skull castings.
SA 26,975	125.2	276.0	Ditto
SA 27,030	134.0	295.5	Ditto
SA 27,109	146.5	323.0	Ditto
SA 27,162	118.0	260.2	Ditto
SA 27,167	125.0	275.6	Ditto
SA 27,171	133.2	293.7	Ditto
SA 27,172	102.5	226.0	electrode was side-gated skull castings, but no nitride seeds were added -- all other electrodes contained synthetic defects.
SA 27,175	121.5	267.9	electrode was an accumulation of left-over parts of side-gated skull castings plus a reclaimed part of a prior remelt that was ruined when the electrode dropped into the pool.

14
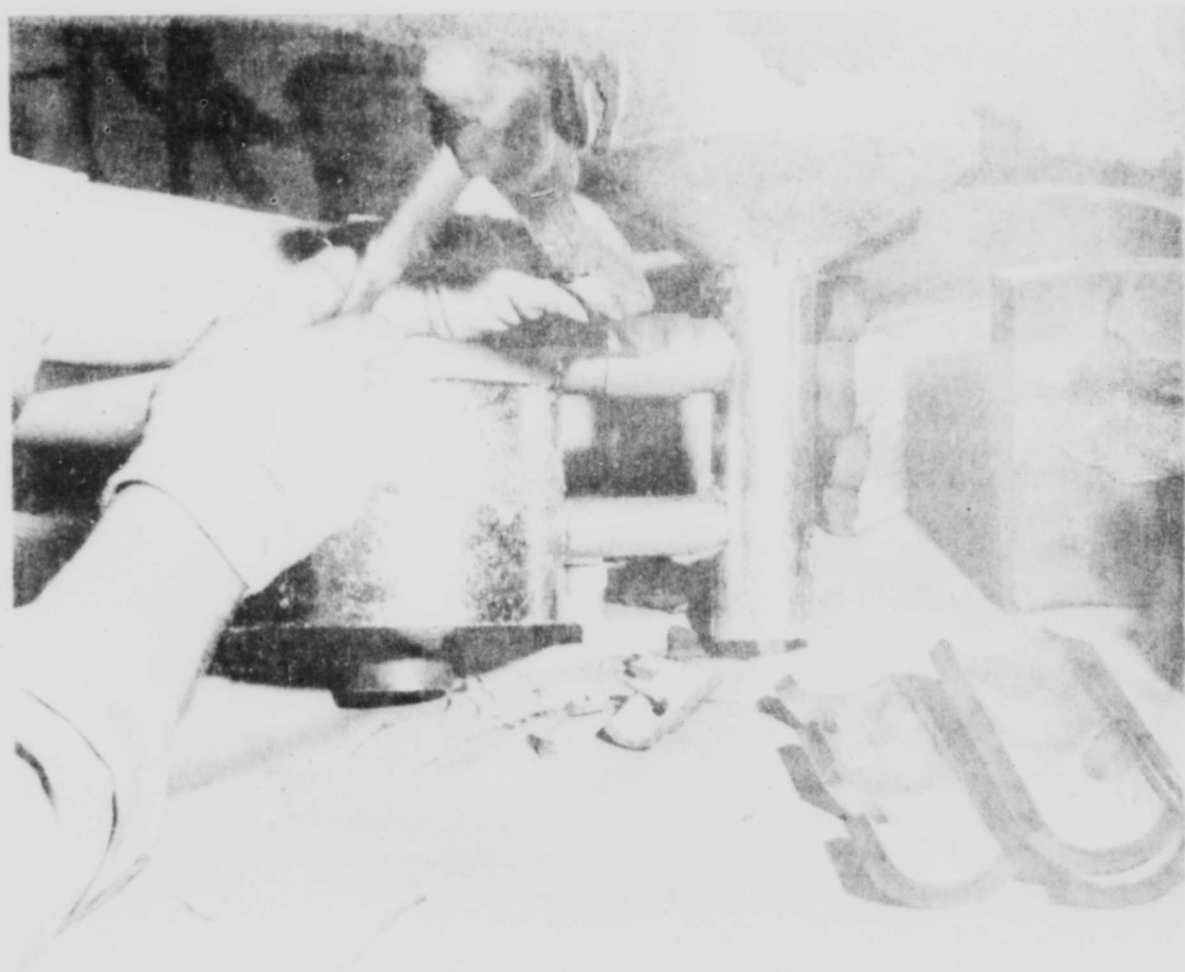
FIGURE 2. - Filled graphite mold

15

FIGURE 3. - Skull casting removed from mold

16
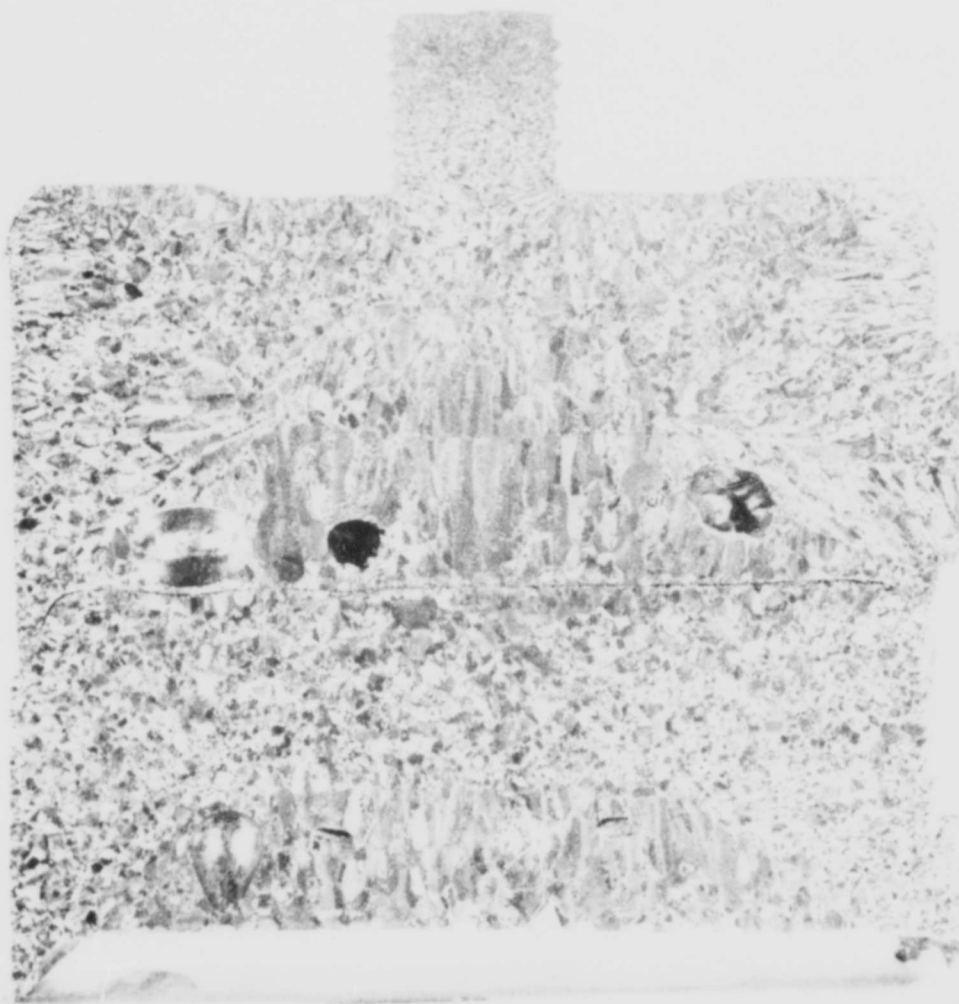
FIGURE 4. - Cross section of a skull-cast ingot
with gates and sprue removed
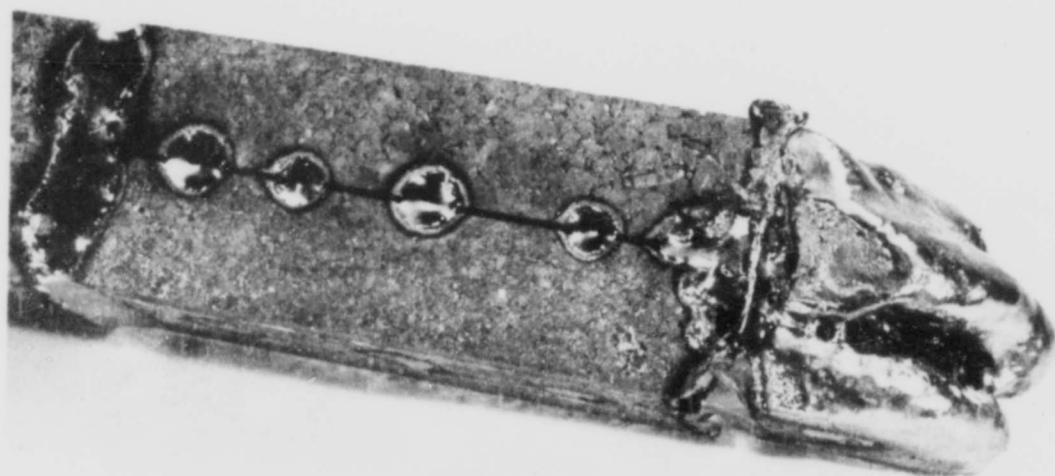
FIGURE 5. - Partly consumed sponge-bar electrode

18

FIGURE 6. - Electrode for remelting

FIGURE 7. - As-cast remelt ingot, crucible, and electrode
stub

FIGURE 8. - One-inch plate converted from a ten-inch remelt ingot

may be counted as representative of the test process involving side-gated skull castings, depending on whether SA 27,175 is included. Actually, evaluation data fail to distinguish the final ingot from the others, but it is an aberration because the electrode history was different. The first ingot, SA 26,869, was made from direct-pour castings, of course. SA 26,917 was a triple melt, and SA 27,172 was an unseeded double melt.

Some additional features of the processing are revealed in Figures 5 through 8. Figure 5 shows the tip of a partially consumed first-melt electrode made from sponge bars. Figure 6 shows an assembled electrode for remelt. This particular electrode includes some sections, at the bottom, being recycled from the top parts of prior 10" remelt ingots. A remelt ingot, the copper crucible in which it was melted, and the stub of the electrode consumed are displayed in Fig. 7. Figure 8 shows the 1" plates rolled from one ingot.

3. RESULTS AND INTERPRETATION

3.1 Ingot Quality

The remelt ingots already have been identified in Table VI and Figure 7 illustrates their typical appearance. Their analyses are summarized in Tables VII and VIII. Nitrogen was added in the form of refractory seeds, of course, and there was some chance of adding carbon from casting molds to the rather high level already contained in the starting sponge (see Table II).

Some of the nitride may have been dissolved. The average nitrogen content of the remelt ingots, excluding SA 27,172, was 166.4 ppm. But SA 27,172, to which no nitride was added, contained only about 120 ppm of dissolved nitrogen, and the average nitrogen content of five samples of

the starting sponge was 134 ppm. A typical 12-bar sponge electrode contained about 12 g of synthetic nitride. Assuming the seeds contained about 15% by weight of nitrogen, the total nitrogen content of an electrode would be about 1.8 g which, if homogeneously dissolved, would contaminate a 30 kg casting to a level of about 60 ppm. The increase indicated by the analyses is 0.5 to 0.75 times this much, and it probably comes from solution of nitrides. Most other potential sources can be discounted. The fact that SA 27,172 contained relatively little nitrogen tends to confirm the basic soundness of melting practices. Samples for nitrogen analyses (Kjeldahl method) were collected by machining which entails a risk of contamination, but again the result for SA 27,172 means that if contamination during sampling was a factor, it was not a factor in all cases. The example of SA 27,172 also discourages the notion that significant nitrogen was added with master alloy (also see Table IV). Thus, the nitrogen contamination seems to be associated with the addition of nitride seeds. However, whether the analytical results actually mean that 50% to 75% of the nitride was dissolved depends on how well the samples represented whole ingots. Since only the outside surfaces were sampled, the distribution of nitrogen inside ingots was not tested, but the surface samples themselves were examined for differences of nitrogen content. Results are summarized in Table IX. Samples that contained the most nitrogen all came from the lower two-thirds of the ingots. However, the high values were intermixed with lower values with the net effect that the scatter of results was about twice as great as in the upper parts. The situation suggests that nitrogen is present in localized concentrations that are included in some samples but not others, and that the chance of including one or more nitrogen-rich pockets in a sample is greater in the lower part of an ingot. In recapitulation, it appears that at least part of the nitride seeds added to the metal resided in remelt ingots as nitrogen-rich patches (not inclusions) which tend to be concentrated low in the ingots. Incidentally, for the unseeded ingot (SA 27,172),

TABLE VII. - Analytical comparison of remelt ingots[1] and electrodes[2] melted into them

Description		Al, %		V, %		C, ppm		N, ppm		Brinell hardness	
		av.	σ	av.	σ	av.	σ	av.	σ	av.	σ
SA 26,869	Electrode	6.01	0.40	4.03	0.16	389.2	47.7	173.5	15.3	314	14.6
	Ingot	6.13	0.16	4.17	0.07	462.0	40.4	159.4	8.7	339	5.2
SA 26,917	Electrode	6.43	0.09	3.98	0.08	--	--	170.5	5.8	---	---
	Ingot	6.47	0.20	4.12	0.43	169.6	43.3	182.6	21.2	350	8.2
SA 26,956	Electrode	6.24	0.26	3.80	0.20	479.2	76.0	169.2	12.0	330	12.6
	Ingot	6.24	0.08	3.87	0.06	534.4	84.3	176.2	9.4	339	11
SA 26,975	Electrode	5.87	0.33	3.92	0.32	516.4	101.6	154.5	17.8	312	15.0
	Ingot	5.77	0.04	3.93	0.11	594.2	84.3	158.6	7.0	317	9.9
SA 27,030	Electrode	5.82	0.20	3.99	0.26	559.4	91.2	145.7	11.6	315	5.5
	Ingot	5.99	0.11	3.96	0.15	421.4	37.9	158.4	4.8	331	14.4
SA 27,109	Electrode	5.87	0.17	3.95	0.15	444	31.8	168	17.7	330	8.1
	Ingot	6.15	0.12	3.98	0.09	422.8	37.9	170.4	12.1	339	15.0
SA 27,162	Electrode	5.94	0.17	4.06	0.12	519	86.7	164	11.6	315	8.5
	Ingot	5.99	0.13	4.04	0.10	512	85.5	165	11.3	331	16.1
SA 27,167	Electrode	5.20	0.14	4.05	0.15	444	44.7	160	14.5	317	14.5
	Ingot	5.59	0.20	3.95	0.06	499	52.8	169	13.3	327	22.5

(Continued)

TABLE VII. - Analytical comparison of remelt ingots[1] and electrodes[2] melted into them (Continued)

Description	Al, % av.	Al, % σ	V, % av.	V, % σ	C, ppm av.	C, ppm σ	N, ppm av.	N, ppm σ	Brinell hardness av.	Brinell hardness σ
SA 27,171 Electrode	5.81	0.19	4.16	0.14	648	92.8	152	8.0	301	7.6
Ingot	6.26	0.17	3.61	0.21	383	33.6	161	6.3	331	7.1
SA 27,172 Electrode	5.72	0.47	3.97	0.14	466	141.2	122	12.9	316	14.6
Ingot	6.23	0.21	3.48	0.22	370	26.1	117	14.4	333	4.0
SA 27,175 Ingot	6.11	0.15	3.94	0.14	387	58.0	163	14.0	329	8.4

[1] Analyses based on 5 samples per remelt ingot.
[2] Analyses based on 2 samples per prior ingot (5 to 8 ingots per electrode).

25

TABLE VIII. - Remelt ingot impurities[1]

Ingot no.	Ca	Cr	Cu	Fe	Mg	Mn	Mo	Ni	Pb	Si	Sn	Y	H[2]	O[2]
SA 26,869	<10	40	<10	30	<5	200	50	<20	<100	300	<100	<50	--	--
SA 26,917	<10	80	50	90	<5	200	80	<20	<100	500	100	<50	23	1,177
SA 26,956	<10	10	<10	20	<5	200	20	<20	<100	200	<100	50	29	823
SA 26,975	<10	30	20	50	<5	500	30	<20	<100	1000	100	100	31	785
SA 27,030	<10	20	20	30	<5	300	40	<20	<100	1000	<100	<50	--	--
SA 27,109	<10	30	100	30	<5	200	20	<20	<100	250	<100	<50	--	--
SA 27,162	<10	10	<10	20	<5	200	30	<20	<100	250	<100	<50	--	--
SA 27,167	<10	20	<10	20	<5	300	30	<20	<100	500	<100	<50	--	--
SA 27,171	<10	20	<10	30	<5	200	20	<20	<100	500	<100	<50	--	--
SA 27,172	<10	10	20	50	<5	200	20	<20	<100	500	<100	<50	45	973
SA 27,175	<10	10	50	20	<5	50	15	<20	<100	90	<100	<50	--	--

[1] Results in ppm.
[2] Samples taken from plate after rolling.

26

TABLE IX. - Nitrogen and carbon contents as functions of sample location

Sample Number	Location	Nitrogen[1] Average	σ	Carbon[2] Average	σ
1	top surface	157.4 ppm	6.80 ppm	486.2 ppm	101.8 ppm
2	upper sidewall	161.8	7.44	484.1	106.4
3	middle sidewall	171.7	11.85	425.8	69.2
4	lower sidewall	171.6	19.39	460.1	86.1
5	bottom surface	169.5	14.54	436.9	62.8
1,2	upper one-third	159.6	7.11	485.2	101.2
3,4,5	lower two-thirds	170.9	14.81	440.9	74.7

[1] Average of ten nitride-seeded ingots.
[2] Average of ten ingots melted from graphite-molded skull castings.

the top-to-bottom sequence of nitrogen values was 104, 105, 112, 130, and 135 ppm. Thus, even this ingot displayed higher nitrogen concentrations toward the bottom. A very similar tendency has been reported (1) for the oxygen content of 95-cm-diameter (37.4") ingots of CP titanium to which oxide was added to meet various sub-grade specifications.

The results of carbon analyses are even more scattered than the nitrogen values. This is evident in Table VII. But despite some individual high values, the overall average of carbon in ingots remelted from skull castings was only 458.6 ppm. This value is on the low side of expectations. If significant carbon was added to the metal in the melting process, it was not shown by the routine sampling and analysis. Nevertheless, different locations were compared for differences of carbon content. The results are shown in Table IX along with the analogous results for nitrogen content. It appears that the distribution of carbon is opposite to the nitrogen distribution. The average carbon content and the scatter of individual values are both higher in the top third rather than the bottom two-thirds of the ingots.

For the sake of comparison, analytical results for Al and V were studied in the manner of Table IX, but in this case the top-to-bottom uniformity was quite good except for low values corresponding to the bottom surfaces of ingots. The average percentages, with standard deviations shown as limits and in top-to-bottom order, were: 6.15 ± 0.29, 6.11 ± 0.33, 6.12 ± 0.24, 6.11 ± 0.22, 5.94 ± 0.20 for the Al content; and 3.96 ± 0.25, 3.95 ± 0.18, 3.96 ± 0.16, 3.97 ± 0.34, 3.73 ± 0.25 for the V content.

Besides compositional analyses, some information about as-cast ingot quality was obtained from nondestructive and destructive examinations. The gist of this information is that the metal seemed to be unusually "gassy"

or "dirty". One clue was a difficulty in penetrating ingots with ultrasound to locate "shrinkage" regions. Ingots were inspected longitudinally and diametrically. Except for the triple-melt ingot (SA 26,917), longitudinal penetration with 5 MHz sound was not possible and 2.25 MHz signals were reflected from the opposite end only through outer metal. Interference was excessive in a core region near the axis. Even for inspection along a diameter, the 2.25 MHz signal was more acceptable. As a result of the ultrasonic inspections, defective metal was removed from the tops of most ingots before they were converted. Two of the removed sections are illustrated in Figures 9 and 10. Typically, about 4 to 4.5 inches of an ingot length were rejected. Clearly, the flaws are gas holes, and it seems significant that the ingot not artificially seeded is essentially as gassy as the rest (see Fig. 10). In contrast, the triple-melt ingot, SA 26,917), contained a relatively small void about an inch below the top surface. It is not clear whether the difference is attributable to the fact that the metal was melted once more, to the fact that skull casting was not involved, or to the fact that the titanium came from a separate lot of sponge.

Another relevant observation resulted from radiography. It has been mentioned that a direct-pour skull casting was cut open, and that nitride inclusions were found inside. Thus a half-inch-thick slice of as-cast metal was available with nitride inclusions at known locations. This slice was radiographed to see if the inclusions could be resolved. They could not, but the as-cast grain structure of the metal slice was clearly visible. Later, a radiograph of the same slice was included in a group submitted for a trial analysis by a color extraction process. These tests were done by the Materials Processing Laboratory of the Philco-Ford Corp., Aeronutronic Division, Newport Beach, California. In the process, a series of photographic masks are prepared, representing "windows" of radiographic density. The masks are then printed in

FIGURE 9. - Polished and etched cross section of metal removed from the top of ingot SA 27,030

FIGURE 10. - Polished and etched cross section of metal removed from the top of ingot SA 27,172

31

contrasting colors, so that regions of slightly different radiographic density can be displayed as markedly different colors. In both the regular radiograph and the color derivation, but especially in the color print, it is evident that the grains are visible because some part of the structure, presumably the grain boundaries, is more transparent to X-rays than the balance of the structure. That is, it appears that grain boundaries have a lower "average" atomic number or a lower effective density than the grains. Furthermore, the effect is not uniform, but is most intense in a central core and fades away near the sidewalls of the casting. The same sort of thing, albeit less intense, could be responsible for the low ultrasonic transmittance of remelt ingots.

3.2 Nondestructive Examination of Rolled Plates

Results of ultrasonically inspecting the rolled plate are summarized in Tables X and XI. The tables contain the same sort of information except that in Table X there was no consideration of apparent flaws shorter than 60 mils long. Table XI is more complete, but Table X is a clearer presentation of most of the trends. Therefore, both presentations seem worthwhile, despite repetition.

The scheme used for evaluation of the data is an adaptation of ASTM Recommended Practice E45-63 (also AMS 2301) for the Magnetic Particle Method of Determining the Inclusion Content of Steel. The essence of the procedure is a numerical weighting of defects according to size.

TABLE X. - Evaluation of ultrasonic inspection record charts, based on
counting of reflecting discontinuities of length >60 mils

Ingot number	Plate section	Frequency, in^{-3}	Total score	Severity rating, in^{-3}	Severity distribution, %
SA 26,869	BT	0.044	56.0	0.353	88.9
	TC	0	0	0	0
	BC	0	0	0	0
	TB	0	0	0	0
	BB	0.018	7.0	0.042	11.1
	all	0.011	63.0	0.071	
SA 26,917	TM	0	0	0	0
	TB	0.018	4.5	0.020	100.0
	all	0.008	4.5	0.009	
SA 26,956	T-TT	0	0	0	0
	B-TT	0	0	0	0
	T-BT	0	0	0	0
	B-BT	0	0	0	0
	T-TB	0.026	6.5	0.042	8.0
	B-TB	0.053	53.0	0.354	64.8
	T-BB	0.047	11.5	0.076	14.2
	B-BB	0.032	10.5	0.068	13.0
	all	0.020	81.5	0.068	

(Continued)

33

TABLE X. - Evaluation of ultrasonic inspection record charts, based on
counting of reflecting discontinuities of length >60 mils

Ingot number	Plate section	Frequency, in^{-3}	Total score	Severity rating, in^{-3}	Severity distribution, %
SA 26,975	TT	0	0	0	0
	BT	0	0	0	0
	TB	0.004	2.0	0.008	6.2
	BB	0.019	31.0	0.120	93.8
	all	0.006	33.0	0.033	
SA 27,030	TT	0.015	2.5	0.007	0.5
	BT	0.426	379.0	1.153	58.8
	TB	0.185	254.5	0.736	39.5
	BB	0.014	6.5	0.019	1.2
	all	0.156	646.5	0.472	
SA 27,109	TT	0.020	4.0	0.011	12.5
	BT	0.009	3.0	0.009	9.4
	TB	0.015	10.5	0.032	33.1
	BB	0.040	14.0	0.040	45.0
	all	0.021	31.5	0.023	
SA 27,162	TT	0	0	0	0
	BT	0.028	15.5	0.061	62.0
	TB	0	0	0	0
	BB	0.034	9.5	0.040	38.0
	all	0.014	25.0	0.024	

(Continued)

34

TABLE X. - Evaluation of ultrasonic inspection record charts, based on counting of reflecting discontinuities of length >60 mils

Ingot number	Plate section	Frequency, in^{-3}	Total score	Severity rating, in^{-3}	Severity distribution, %
SA 27,167	TT	0	0	0	0
	BT	0	0	0	0
	TB	0	0	0	0
	BB	0.007	2.5	0.009	100.0
	all	0.002	2.5	0.002	
SA 27,171	TT	0	0	0	0
	BT	0.003	1.0	0.003	3.2
	TB	0.018	17.0	0.052	57.7
	BB	0.027	11.5	0.035	39.1
	all	0.011	29.5	0.022	
SA 27,172	TT	0.013	3.5	0.011	100.0
	TC	0	0	0	0
	BB	0	0	0	0
	all	0.005	3.5	0.004	
SA 27,175	TT	0	0	0	0
	BT	0	0	0	0
	TB	0.025	22.5	0.081	55.7
	BB	0.014	18.0	0.063	44.3
	all	0.010	40.5	0.037	

TABLE XI. – <u>Evaluation of ultrasonic inspection record</u>
<u>charts, based on counting of reflecting</u>
<u>discontinuities of length >20 mils</u>

Ingot number	Plate section	Frequency, in^{-3}	Total score	Severity rating, in^{-3}	Severity distribution, pct.
SA 26869	BT	0.057	56.375	0.355	88.2
	TC	0.005	0.125	0.001	0.2
	BC	0	0	0	0
	TB	0.006	0.125	0.001	0.2
	BB	0.036	7.375	0.044	11.4
	all	0.019	64.000	0.072	
SA 26917	TM	0.039	1.375	0.005	13.7
	TB	0.150	8.750	0.039	86.3
	all	0.089	10.125	0.020	
SA 26956	T-TT	0.027	0.500	0.003	0.6
	B-TT	0.007	0.125	0.001	0.2
	T-BT	0.007	0.125	0.001	0.2
	B-BT	0.006	0.125	0.001	0.2
	T-TB	0.110	8.500	0.055	9.5
	B-TB	0.174	55.875	0.373	61.8
	T-BB	0.133	13.250	0.088	14.8
	B-BB	0.071	11.375	0.074	12.7
	all	0.067	89.875	0.075	
SA 26975	TT	0.008	0.250	0.001	0.5
	BT	0	0	0	0
	TB	0.012	2.375	0.009	6.5
	BB	0.039	31.875	0.123	93.0
	all	0.015	34.500	0.034	
SA 27030	TT	0.276	14.375	0.042	2.1
	BT	1.153	414.250	1.261	58.3
	TB	0.506	266.875	0.772	37.5
	BB	0.091	14.375	0.041	2.1
	all	0.497	713.250	0.521	

(Continued)

36

TABLE XI. - Continued:

Ingot number	Plate section	Frequency, in^{-3}	Total score	Severity rating, in^{-3}	Severity distribution, pct.
SA 27109	TT	0.218	13.125	0.037	12.8
	BT	0.356	18.125	0.055	17.4
	TB	0.286	22.000	0.068	21.3
	BB	0.823	50.375	0.143	48.5
	all	0.424	103.625	0.076	
SA 27162	TT	0.068	2.500	0.009	6.4
	BT	0.091	17.875	0.071	47.3
	TB	0.109	4.000	0.014	10.3
	BB	0.174	13.625	0.058	36.0
	all	0.109	38.000	0.036	
SA 27167	TT	0.041	1.500	0.005	16.0
	BT	0.017	0.625	0.002	6.5
	TB	0.018	0.625	0.002	6.3
	BB	0.116	6.625	0.023	71.2
	all	0.047	9.250	0.008	
SA 27171	TT	0.073	3.000	0.009	6.5
	BT	0.095	5.750	0.017	12.9
	TB	0.067	19.125	0.058	42.0
	BB	0.165	17.750	0.053	38.6
	all	0.099	45.625	0.034	
SA 27172	TT	0.344	16.875	0.054	50.4
	TC	0.218	8.000	0.028	23.7
	BB	0.257	8.750	0.033	25.9
	all	0.276	33.625	0.039	
SA 27175	TT	0.004	0.125	negligible	0
	BT	0.015	0.500	0.002	1.0
	TB	0.223	29.875	0.108	56.7
	BB	0.134	22.375	0.079	42.3
	all	0.095	52.875	0.048	

37

The weighting factors used for Tables X and XI are listed below:

Length of apparent flaw	Weight factor	Length of apparent flaw	Weight factor
>0.020" to 1/32"	1/8	>1/2" to 3/4"	4
>1/32" to 1/16"	1/4	>3/4" to 1"	8
>1/16" to 1/8"	1/2	>1" to 2"	16
>1/8" to 1/4"	1	>2"	32
>1/4" to 1/2"	2		

Of course, the reflection of an ultrasonic signal does not in itself identify the character of the reflecting interface. Thus all indications in a given size group had to be treated equally without regard for the cause of reflection. The lengths of reflecting discontinuities were estimated by comparison with flat-bottomed test holes ranging in size from 0.010" to 1".

To obtain the tabulated results, all indications above a specified minimum size were counted. The "frequency" is just the number counted, regardless of size, divided by the approximate volume of metal represented. The number in each size group was weighted with the appropriate factor and the sub-scores thus assigned were summed to get the "total score". The "severity rating" is the total score divided by the volume of metal represented, and it might be thought of as a weighted frequency. Finally, the "severity distribution" is the relative contribution of each section of metal, taking volume differences into account, to the overall severity rating of the ingot.

Sections of plate from each ingot are listed in top-to-bottom order. For ingots SA 26,869 and SA 26,917, the plate sections designated TT were omitted from the tabulations because they corresponded to the defective regions cropped from the tops of other ingots. The plate SA 26,869-BT corresponds roughly to the TT sections of most other ingots, and the plate SA 26,917-TM corresponds to a combination of TT and BT sections for most other ingots.

The severity ratings are broadly distributed, but the overall ratings for ingots seem to fall into ranks as shown in Table XII. The "dirtiest" ingot was SA 27,030, and the "cleanest" was SA 27,167 although it is not really distinguishable from the unseeded ingot, SA 27,172, if indications <60 mils are ignored. It is interesting that the unseeded ingot apparently was not completely clean, especially with respect to small indications. It is also interesting that the triple-melt ingot had a fairly clean ranking. There are no obvious reasons, in terms of processing or materials variations, for the wide spread of severity ratings (0.002 to 0.472 in^{-3} in Table X) among the seeded ingots, all produced from side-gated castings.

Despite the spread of severity ratings, there was some consistency in the severity distribution. Among the seeded ingots that involved side-gating, there was clearly a better chance of finding clean metal at the top of an ingot (after cropping the shrinkage region). This is emphasized in Table XIII where data selected from Table X are redisplayed. The tendency is reminiscent of the nitrogen enrichment of the lower parts of ingots, described in an earlier section of this report. However, ingot SA 26,869 and the unseeded ingot, SA 27,172, both were ultrasonically cleaner in their lower parts even though they contained more nitrogen there.

An effort was made to check some of the ultrasonic results by using X-ray radiography. The task was not completed, but selected sections of plates SA 26,869

TABLE XII. - Ranking of ingots according to severity ratings

Rank	Range of overall severity rating, in⁻³	Ingots in each rank	
		Indications <60 mils excluded (see Table X)	Indications <60 mils included (see Table XI)
A	<0.005	SA 27,167, SA 27,172	None
B	0.005 to 0.015	SA 26,917	SA 27,167
C	0.020 to 0.050	SA 26,975, SA 27,109 SA 27,162, SA 27,171 SA 27,175	SA 26,917, SA 26,975, SA 27,162, SA 27,171, SA 27,172, SA 27,175
D	0.065 to 0.080	SA 26,869, SA 26,956	SA 26,869, SA 26,956, SA 27,109
E	0.450 to 0.550	SA 27,030	SA 27,030

TABLE XIII. - Distribution of severity for apparent flaws >60 mils in ingots produced from side-gated skull castings

Ingot No.	Plate Identification			
	TT	BT	TB	BB
SA 26,956	0	0	72.8%	27.2%
SA 26,975	0	0	6.2	93.8
SA 27,030	0.5%	58.8%	39.5	1.2
SA 27,109	12.5	9.4	33.1	45.0
SA 27,162	0	62.0	0	38.0
SA 27,167	0	0	0	100.0
SA 27,171	0	3.2	57.7	39.1
SA 27,175	0	0	55.7	44.3
Average	1.6	16.7	33.1	48.6

(TT, BT, TC, TB, and BB), SA 26,917 (TT), SA 26,956 (T-TB, B-TB, T-BB, and B-BB), SA 26,975 (TB and BB), and SA 27, 030 (BT) were radiographed. Thus, radiographs were obtained for all sections of SA 26,869 and the ultrasonically dirtiest parts of the other ingots listed. For ingots SA 26,869, SA 26,956, and SA 26,975, the radiographs generally confirmed results of ultrasonic inspection except that the radiography failed to resolve apparent defects unless they were more than about 100 mils in size, despite a lack of difficulty in resolving 40-mil penetrameter holes. In contrast, for ingots SA 26,917 and SA 27,030, radiographs contained no evidence of flaws. This latter result was especially surprising in the case of SA 27,030.

Two radiographs, representing parts of plates SA 26,869 (TT and BT) were analyzed by the color extraction method described earlier. The only new information resulting from this treatment was a shading around flaws, indicative of a zone of slightly enhanced radiographic transparency. Subsequent metallography and microprobe analyses of the particular flaws involved showed that the primary flaws were nitrogen-rich inclusions, but with minimal reaction zones of nitrogen content <0.5% by weight. The shading revealed by the color analysis presumably was a differentiation of the low-nitrogen regions. If so, it was an interesting accomplishment.

3.3 Preliminary Metallography

Metallography was not initially planned as a major part of the investigation. Nevertheless, as an adjunct, it was useful in identifying or attempting to identify the causes of nondestructive flaw indications. Metallographic specimens were taken from plates SA 26,869 (TT, BT, and BB), SA 26,917 (TT and BB), SA 26, 956 (T-TB, B-TB, T-BB, and B-BB), SA 26,975 (TB and BB), SA 27,030 (TB and BB), SA 27,162 (BB), and SA 27,172 (TT). These were examined optically, and many were analyzed with an electron microprobe.

42

Nitrogen-rich inclusions (Type I defects) were found in five ingots as represented by ten plates: SA 26,869 (TT and BT), SA 26,956 (T-TB, B-TB, T-BB, and B-BB), SA 26,975 (TB and BB), SA 27,030 (BB), and SA 27,162 (BB). Except for one inclusion in the top part of SA 26,869, all of the inclusions were found in metal from the bottom parts of ingots. Although no two inclusions are exactly alike, they cannot all be illustrated here. Instead, four examples have been selected. Figure 11 is unusual because it shows an inclusion still attached to surrounding metal. More often, the inclusion is detached. It is estimated that in the as-cast ingot, the illustrated defect would have been located about 3 to 3.5 inches from the bottom. This particular specimen exhibits a sequence of five separate zones of structure, ranging from the spongy bulk of the inclusion to the matrix structure. Compositional differences for the sequence of structures, based on two separate microprobe surveys, are listed in Table XIV.

Figure 12 shows a large inclusion with a seam or vein of contrasting material running through it. The specimen is from a location that should have been about 1 to 1.5 inches from the top of an as-cast ingot that was not cropped to eliminate the shrinkage region. In other words, the defect is from the shrinkage region of the ingot. The material in the seam contained about 12% N and 1.8% V, and the material outside contained about 16% N and 0.5% V. The difference in vanadium content is probably more significant than the difference of nitrogen content. Another inclusion with a contrasting seam through it is shown in Figure 13. Apparently, this structural feature is not uncommon. Neither is the occurrence restricted to a particular part of an ingot. This example was formed about 4 to 4.5 inches from the ingot bottom. Figure 14 illustrates an acicular structure sometimes exhibited by inclusions instead of the spongier structure
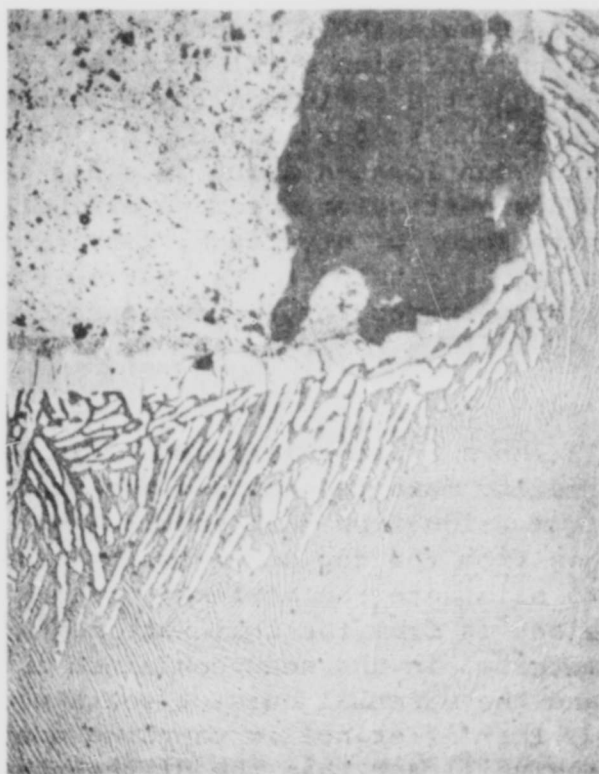
FIGURE 11. - Micrograph (originally 100X) of specimen R12,
mount F992, from plate SA 26,975-BB

TABLE XIV. – Analyses of zones due to anisomorphous diffusion of a nitride inclusion into a Ti-6Al-4V matrix

Structure	N, %		Al, %		V, %	
	a	b	a	b	a	b
Inclusion, spongy bulk	11.5	14	<0.1	0.6	*	0.3
Thin acicular band at outside edge of inclusion	6.7	11	0.6	0.1	0.5	1.0
Snooth case outside of inclusion	2.3	1.8	5.0	3.9	1.4	1.1
Transition zone with α platelets, some extending from case	0.5	1.3	5.0	5.3	3.3	1.3
Matrix	*	*	5.6	5.7	4.0	3.1

* = Not detectable.

45
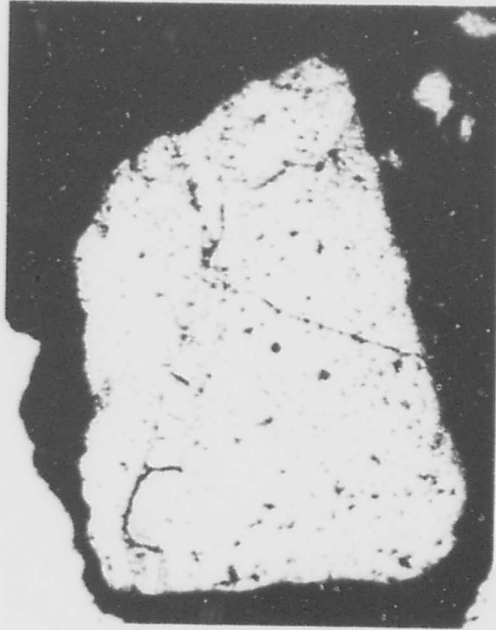
FIGURE 12. - Micrograph (originally 50X) of specimen R4,
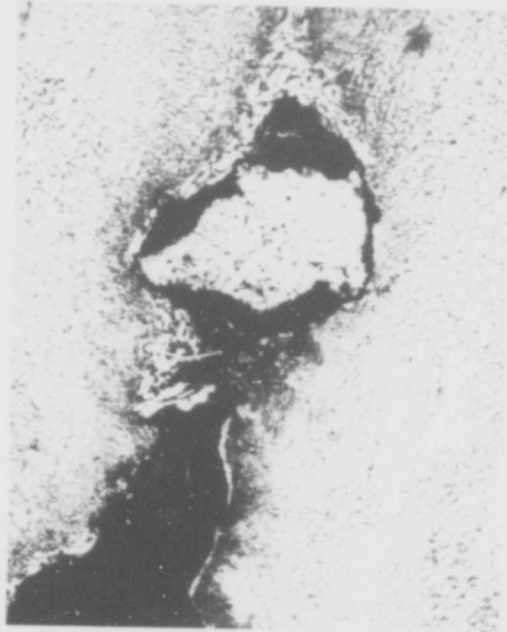mount F763, from plate SA 26,869-TT

FIGURE 13. - Micrograph (originally 50X) of specimen R11, mount F991, from plate SA 26,975-BB

FIGURE 14. - Micrograph (originally 50X) of specimen R25, mount F1092, from plate SA 26,956-B-TB

already mentioned. It represents a site that should have been about 5.5 to 6 inches from the bottom of the as-cast ingot. Microprobe analysis of this inclusion indicated about 9.5% N, a trace of Al, and no V. The nitrogen content is near the stoichiometry of Ti_3N (8.9% N) that has been identified with the epsilon-phase nitride of titanium (5). However, the epsilon-phase stoichiometry has also been specified as Ti_2N (12.7% N) (4).

In addition to the discrete nitride inclusions, at least four other types of flaws were identified by metallography. Figures 15, 16, and 17 show α-stabilized regions contaminated by nitrogen at a relatively low level, but without distinct inclusions. Specimens R15 and R37 (Figs. 16 and 17) were brittle enough to crack during conversion, but specimen R27 (Fig. 15) did not. The maximum nitrogen content observed was 1.3% for R27, 1.2% for R15, and 1.5% for R37. There were minor deficiencies of Al and V at some sites within the stabilized regions. The estimated positions in as-cast ingots were about 6.5 to 7 inches from the bottom for R27, 2 to 2.5 inches from the bottom for R15, and 1 to 1.5 inches from the bottom for R37. Defects of this sort were designated Type II in reference (7).

Another flaw is shown in Figure 18. This is an Al-rich stringer which occupied a position that would have been about 0.5 inch from the bottom of the as-cast ingot. Analysis of a point near the center of the stringer indicated 12.2% Al, 1.2% V, and <0.5% N. Similar defects containing 8 to 9% Al in Ti-6Al-4V matrices have been reported previously (2,6), so the occurrence is not unique.

Figure 19 shows an α-stabilized stringer for which no compositional irregularities were detectable. Of course, with regard to nitrogen, this means only that any
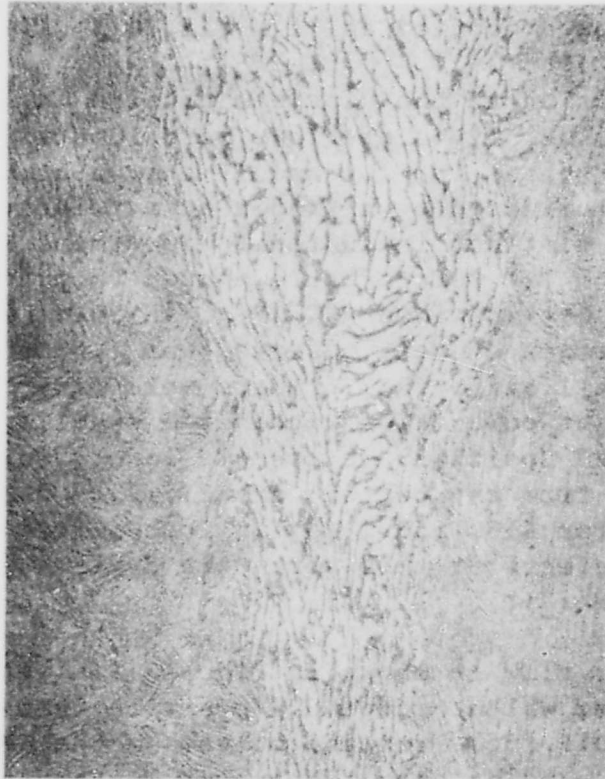
FIGURE 15. - Micrograph (originally 100X) of specimen R27,
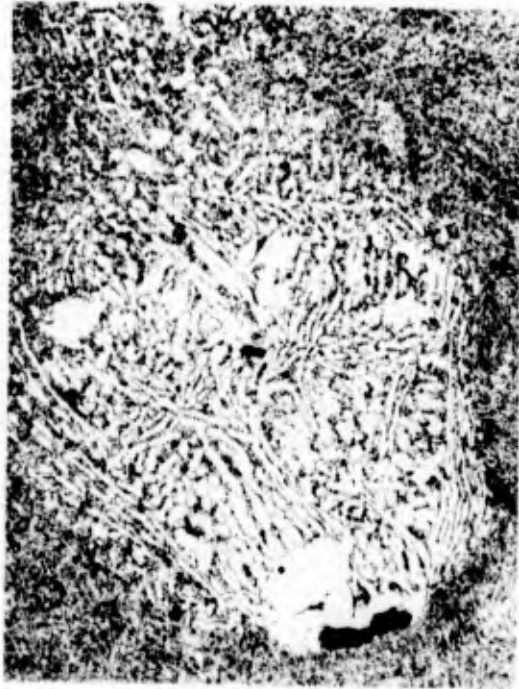mount F1094, from plate SA 26,956-B-TB

FIGURE 16. - Micrograph (originally 50X) of specimen R15,
mount F995, from plate SA 26,975-BB

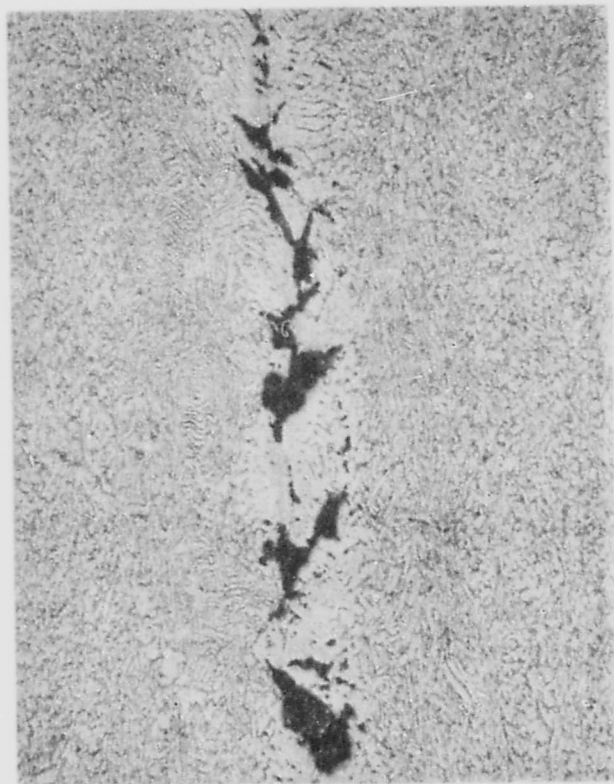FIGURE 17. - Micrograph (originally 50X) of specimen R37, mount F1288, from plate SA 26,917-TB

FIGURE 18. - Micrograph (originally 100X) of specimen R2, mount F761, from plate SA 26,869-BB
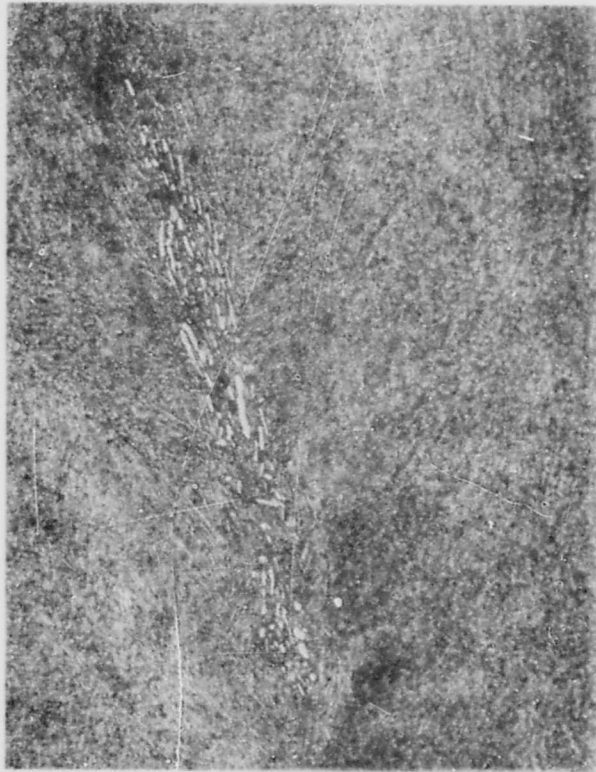
FIGURE 19. - Micrograph (originally 100X) of specimen R16,
mount F996, from plate SA 26,975-BB

contamination was below the detection limit of 0.5%. But this was also true of many of the similar-appearing α-stabilized structures in the reaction zones around nitride inclusions. Thus the defect may be another manifestation of nitride seeding. As usual, the specimen was found in plate from the lower end of an ingot, at a point that would have been about 2 to 2.5 inches from the bottom.

The last specific type of flaw that will be mentioned here appeared as small voids without any α-stabilization, and without any obvious compositional irregularities. In fact, they seemed to be associated with β-rich regions. An example is shown in Figure 20. This one and several others were found in metal that came from the bottom 0.5 inch of the triple-melt ingot. They seemed to be rarer in other ingots.

The presence of a variety of defect types complicated attempts to judge the quality of ingots. However, it was more confounding to be unable to find any flaws at all in many of the locations indicated by nondestructive tests. This happened for eight metallographically mounted specimens from five plates representing five ingots. In addition, several saw cuts were made through plates with the expectation of intersecting flaws, but nothing was revealed and in most cases, no metallographic specimens were removed. The destructive examination encompassed six ingots that had been seeded with nitride. These had been converted to 29 plates of which 13 were virtually clean according to nondestructive tests. Fourteen of the remainder were sectioned and eleven of them, representing six ingots, contained at least one N-rich defect. One other contained identifiable defects of another kind. Thus, in two of the sectioned plates, no defects could be found. However, even in plates where flaws were found, attempts to verify defects at some of the other indicated sites were unsuccessful. The most frustrating example was ingot SA 27,030. Despite ultrasonic evidence of very

FIGURE 20. - Micrograph (originally 50X) of specimen R38,
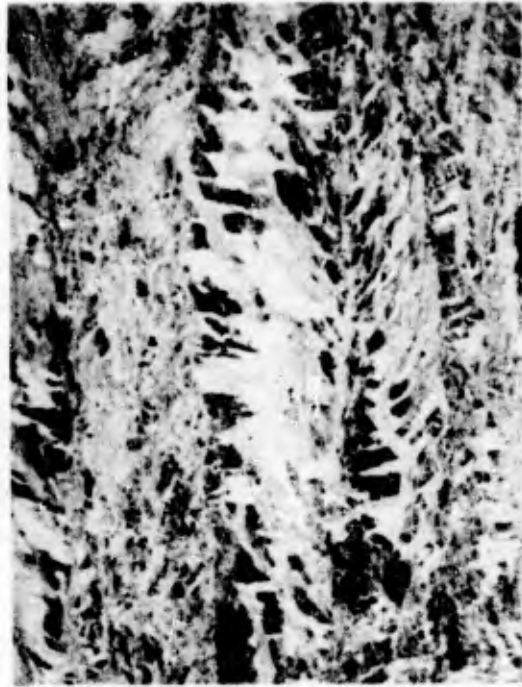mount F1289, from plate SA 26,917-TB

FIGURE 21. - Unusual transverse microstructure (originally 50X), specimen R43, mount G21, from plate SA 27,030-TB
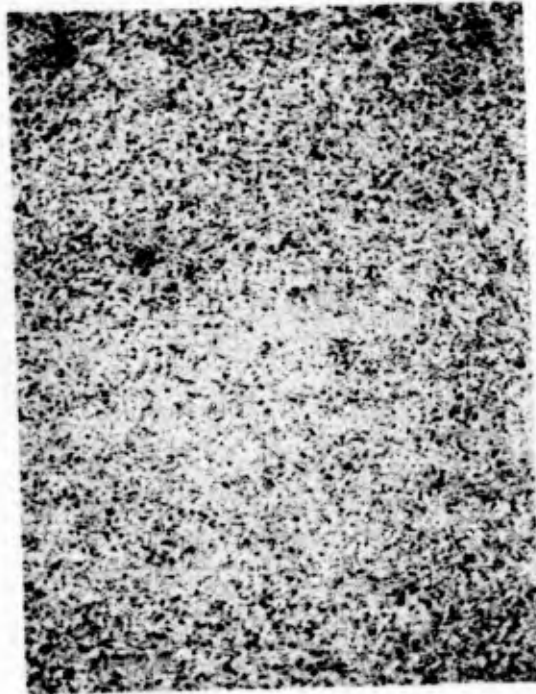
FIGURE 22. - Matrix microstructure (transverse, originally 50X), plate SA 26,869-BB

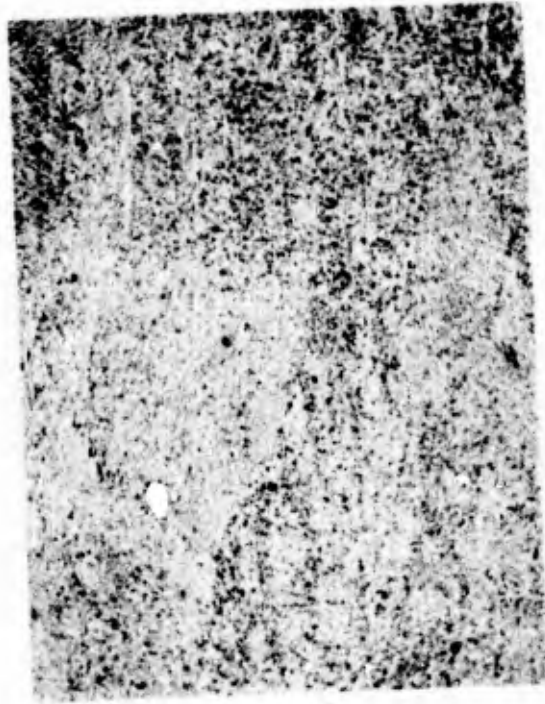FIGURE 23. - Matrix microstructure (transverse, originally 50X), plate SA 26,975-TB

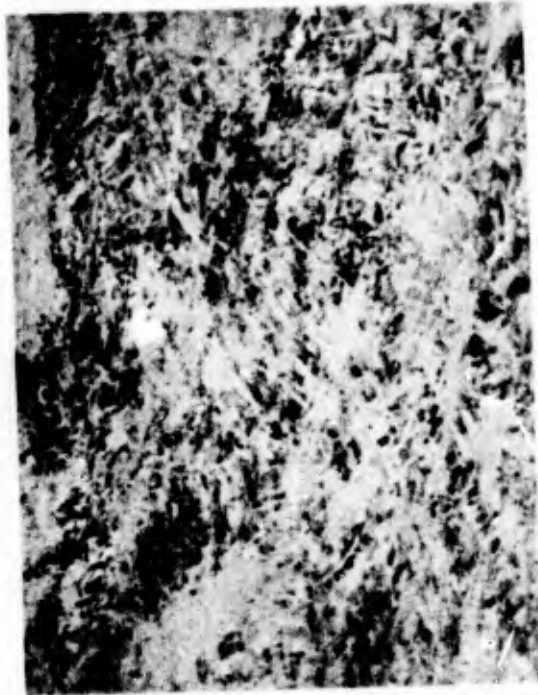FIGURE 24. - Matrix microstructure (transverse, originally 50X), plate SA 27,172-TT

FIGURE 25. - Matrix microstructure (transverse, originally 50X), plate SA 27,030-TB

FIGURE 26. - Matrix microstructure (transverse, originally 50X), plate SA 26,956-B-TB

FIGURE 27. - Matrix microstructure (longitudinal, originally 50X), plate SA 27,162-BB

FIGURE 28. - Matrix microstructure (transverse, originally
50X), plate SA 26,917-TB

many flaws, only one was found metallographically. The confirmed defect was a nitride inclusion and its position, related back to the as-cast ingot, was about 4 to 4.5 inches from the bottom. Other prominent indications of flaws in the plate from the bottom of the ingot could not be confirmed. The plate SA 27,030 (TB) contained 64 flaws >60 mils according to the ultrasonic inspection. Of these, 7 appeared to be more than an inch long and 2 appeared to be more than 2 inches long. Saw cuts were laid out to intersect each of the two largest flaws plus numerous smaller ones. The closest thing to a flaw that could be found metallographically was the sort of structural anomaly shown in Figure 21. Incidentally, results of destructively examining plate SA 27,172 (TT) from the unseeded ingot were similar. Indicated flaws were not verified, but a few structural oddities, similar in appearance but smaller than the one in Figure 21, were found.

One more kind of information was obtained by preliminary metallography. There were some definite differences in matrix structures, as shown in Figures 33 through 28. The illustrations are arranged roughly in order of increasing prominence of prior beta grains and coarseness of alpha. The differences are most likely due to a relative shifting of the $\beta : (\alpha+\beta)$ transus and the thermal conditions of mechanical conversion. Ingot SA 26,869 is known to have been completely converted in the $\alpha+\beta$ range, so the equiaxed α with transformed β structure (Fig. 22) is explainable in that case. However, for the rest of the ingots, it is uncertain whether thermomechanical conditions were too variable or compositional differences actually shifted the transus.

3.4 Extended Examination of Defects

More insight into the nature and causes of defects was sought by continuing the examination of details. Metallographic specimens were prepared from all sites where

65

ultrasonic inspection indicated defects larger than one-half inch long, except that plates rolled from SA 27,030 contained so many apparent defects that they were not all investigated. The defects found were differentiated according to structure, and microprobe analyses were made to establish the composition of the defect and, in the case of inclusion-type defects, the reaction zone around the inclusion.

Some information about the distribution of defects was given in Tables X, XI, and XIII. These results are supplemented by data listed in Table XV. Since the program was primarily directed toward the study of the effect of melting on nitride inclusions, their distribution was separately determined and is listed in Table XVI. The number of defects indicated on ultrasonic charts for sections TB and BT of ingot SA 27,030 have not been included in these tables. There were numerous indications of defects on the ultrasonic charts for these sections, but sawing into defect areas did not reveal any included material or cracks. As was pointed out earlier, defects were most often found in the bottom section of an ingot. This was true not only of nitride-type inclusions, but of all types of defects found.

The primary defects found were of the nitride-inclusion type. These generally consisted of a void with some fragments of the inclusion material still present. The area around the void contained zones of stabilized alpha phase. Typical examples of this type of defect are shown in Figures 29 and 30. The matrix in Figure 29 is normal alpha-beta structure and that of Figure 30 has a worked beta structure. Some slight modifications of this structure were found. Figure 31 shows a nitride inclusion with a solid band of reacted material along one side. The electron probe analyses of this band showed that the fragments of the inclusion contain 10 to 12% nitrogen and less than 0.2% Al and 0.3% V. The equiaxed structure at the edge of the hole is similar to the fragments. The acicular structure is no doubt a mixture of phases but

66

TABLE XV. - Location of most prominent defect indications in remelt ingots

Ingot number	Defects/section				Total
	BB	TB	BT	TT	
SA 26,956	2	3	0	0	5
SA 26,975	1	0	0	0	1
SA 27,030	2	–	–	0	2
SA 27,109	1	1	1	0	3
SA 27,162	3	4	0	0	7
SA 27,167	1	0	0	0	1
SA 27,171	4	3	4	0	11
SA 27,172	0	0	0	2	2
SA 26,869	2	0	5	2	9
SA 27,175	4	2	0	0	6
SA 26,917	0	0	0	1	1
TOTAL	20	13	10	5	48

TABLE XVI. - Distribution of most prominent inclusions with alpha-stabilized reaction zones

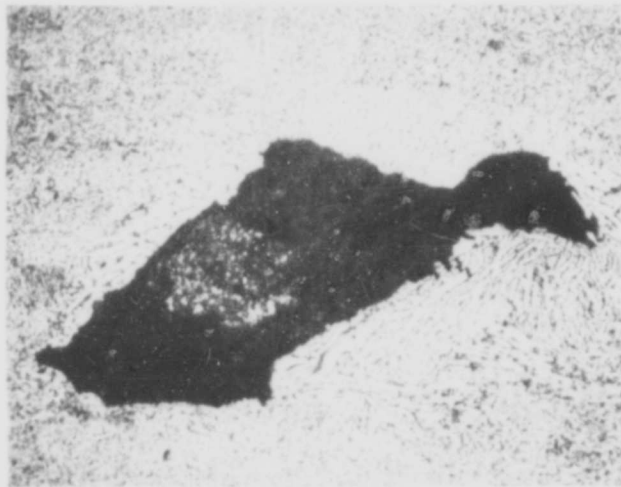| Ingot number	Defects/section				Total
	BB	TB	BT	TT	
SA 26,956	2	3	0	0	5
SA 26,975	1	0	0	0	1
SA 27,030	2	–	–	0	2
SA 27,109	1	1	1	0	3
SA 27,162	2	2	0	0	4
SA 27,167	0	0	0	0	0
SA 27,171	4	3	0	0	7
SA 27,172	0	0	0	0	0
SA 26,869	2*	0	5	2	9
SA 27,175	3	1	0	0	4
SA 26,917	0	0	0	0	0
TOTAL	17	10	6	2	35

*Stringers.

67

FIGURE 29. - Nitride-type inclusion with stabilized α
zone. Normal α-β matrix structure.
(Originally 50X) Specimen R-67, Mount G 410,
from plate SA 27,171-BB.

68

FIGURE 30. - Nitride-type inclusion with stabilized α
zone. Worked β matrix structure.
(Originally 50X) Specimen R-59, Mount G 347,
from plate SA 27,109-TB.

FIGURE 31. - Reaction zone associated with nitride inclusion
(Originally 200X) Specimen R-70, Mount G 413
from plate SA 27,171-BB.

70

the structure is too fine for quantitative analyses of individual phases. Average nitrogen content of this structure decreases from the inside toward the matrix. Nitrogen content of the smooth band is about 3.2% at the inside and decreases to about 0.8% where alpha and beta titanium coexist. The alpha titanium adjacent to the band contains about 0.8% nitrogen while the beta contains less than 0.3% nitrogen.

In some instances, when specimens of a large defect area were examined, only small zones of stabilized alpha or zones of stabilized alpha and small voids were found, as shown in Figure 32. It may be that these were part of a larger defect of the type described above. In fact, in some cases, it was possible to locate the major defect by examining the adjacent material. But there were other cases where isolated alpha stabilizations could not be associated with any inclusion.

The structure shown in Figure 33, although it has the alpha-stabilized zone around a void area, does not appear to be of the same type as the defects described above. It is possible that this defect was due to nitrogen contamination from some source other than seeding, or the different appearance may be related to the relatively low temperature maintained during break-down forging of this particular metal (SA 26,869). The defect is more elongated and broken up than those normally seen.

Three examples of carbide-type inclusions were found in the same ingot, SA 27,162. These are characterized by the absence of a reaction zone of stabilized alpha around the defect. The structure of the surrounding material was that of a worked-beta structure around the two defects found in section TB and a partially broken-up Widmanstätten structure around the one in section BB. Microprobe analyses were made on the inclusion and on the edge of the defect. These data are shown in Table XVII. The carbon content of the inclusions found in section TB is stoichiometric
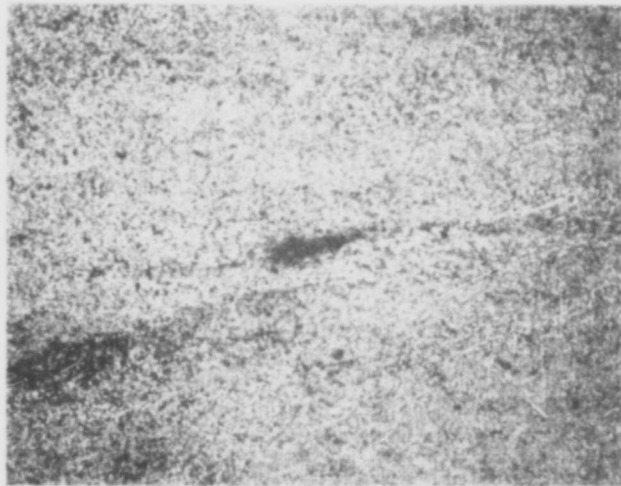
71

FIGURE 32. - Small void with α-stabilized zone.
(Originally 50X) Specimen R-68, Mount G 411,
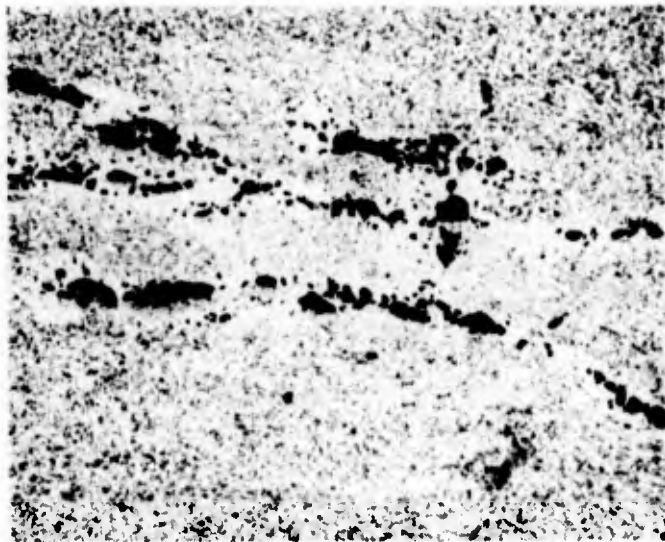from plate SA 27,171-BB.

FIGURE 33. - Elongated nitride inclusion.
(Originally 50X) Specimen R-9, Mount F 933,
from plate SA 26,869-BB.

TABLE XVII. - Microprobe analyses of carbide defect areas

Sample number	Source	Location	C	N	Al	V	Ti
R-64	SA 27,162-BB	Inclusion	13	<.3	<.2	<.5	85
R-64		Hole edge	0.1	<.3	6.0	4.0	90
R-63	SA 27,162-TB	Inclusion	20	<.3	<.2	<.5	80
R-63		Hole edge	0.2	<.3	6.0	4.0	90
R-62	SA 27,162-TB	Inclusion	21	<.5	0.4	0.6	78
R-62		Hole edge	0.7	<.5	4.9	3.6	91

for TiC, but the carbon content for the other inclusion is less than stoichiometric. There appears to be a significant difference in carbon content in the material around the defects. One showed a content of 0.7% while the other two contained 0.1 and 0.2% carbon. Analyses also showed that the carbide is essentially void of the alloying elements. This indicates that the inclusion entered the melt as a carbide and did not form from the reaction of alloy with carbon or graphite which could have come from a casting mold. It may be significant that the sponge starting material for this investigation was unusually rich in carbon (see Table II).

Figures 34, 35, and 36 are photomicrographs of the carbide inclusions. All show the absence of an alpha-stabilized zone, but some differences are apparent. Figure 34 has one large defect with many small carbide particles in the surrounding area. These small carbides are not found in the other two. The defect area shown in Fig. 35 does not appear to be deformed as much as the other two. This could be due to the higher carbon content, 0.7%, which hardened the surrounding material so that it deformed less during conversion.
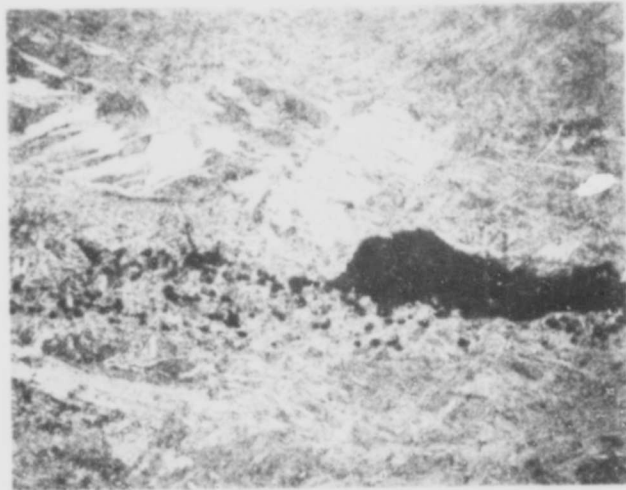
FIGURE 34. - Carbide inclusion with small carbide particle
in matrix. (Originally 50X)
Specimen R-62, Mount G 355,
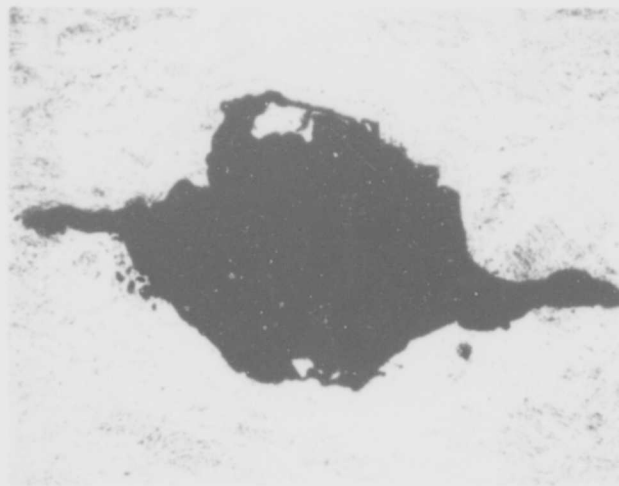from plate SA 27,162-TB.

FIGURE 35. - Carbide inclusion with high carbon content
in surrounding material. (Originally 50X)
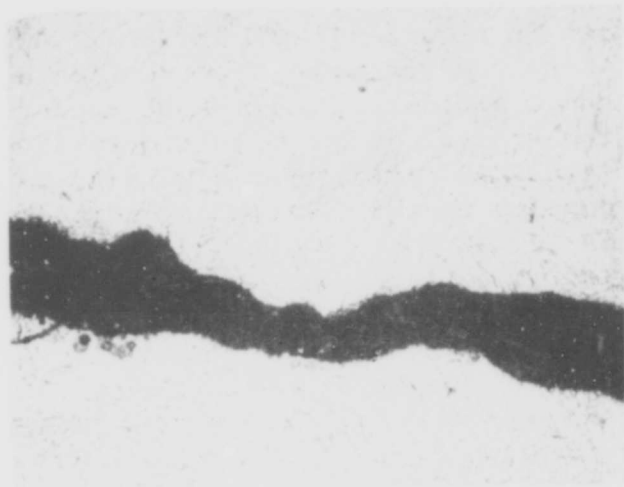Specimen R-63, Mount G 356,
from plate SA 27,162-TB.

FIGURE 36. - Carbide inclusion without α-stabilized zone.
(Originally 50X) Specimen R-64, Mount G 367,
from plate SA 27,162-BB.

In seven cases where the ultrasonic inspection indicated a large defect, no definite inclusion was located. Instead, the material had a worked-beta structure consisting of partially deformed acicular alpha plus beta, with distorted prior beta grain boundaries. Figure 37 is typical of the microstructure found in most of the cases. This structure was found in section BT of ingot SA 27,171 and in the section TT of ingot SA 27,172, the unseeded ingot. It was also found in section BT of SA 27,030, the ingot that had numerous indications of defects in sections BT and TB that could not be confirmed by repeated sawing through suspect areas. The microstructure for SA 27,030 (BT) is shown in Figure 38, and for SA 27,030 (TB) in Figure 21. The "defect area" from section BB of ingot SA 27,167 had a similar structure but appears to be worked less than the others, as shown in Figure 39. The microstructure itself did not appear always to cause the indication of defects on the ultrasonic charts since other material, SA 27,030 (BB), which had this structure showed no indication of defects other than in areas with inclusions.

Specimens for macroscopic examination were prepared from "defect-free" material from SA 27,030 (BB) and from the "defect area" of section TB of the same ingot. Comparison of the structures in Figures 40 and 41 shows that the material from the "defect area", Figure 40, has large grains near the center of the plate and fine grains near the surface, but the material from the "defect-free" area, Figure 41, is uniform throughout. The difference in grain size in the "defective" material is apparently enough to cause an indication of a defect on the ultrasonic trace. Other specimens from ingots SA 26,917 (TT) and SA 27,171 (TB) also showed this difference in grain size in "defect areas" where no inclusions were located. It seems that the duplex macrostructure is a more likely cause of spurious defect indications than the coarse microstructure described in the preceding paragraph.

FIGURE 37. - Worked β structure.   (Originally 50X)
Specimen R-74, Mount G 430,
from plate SA 27,171-BT.

79

FIGURE 38. - Worked β structure. (Originally 50X)
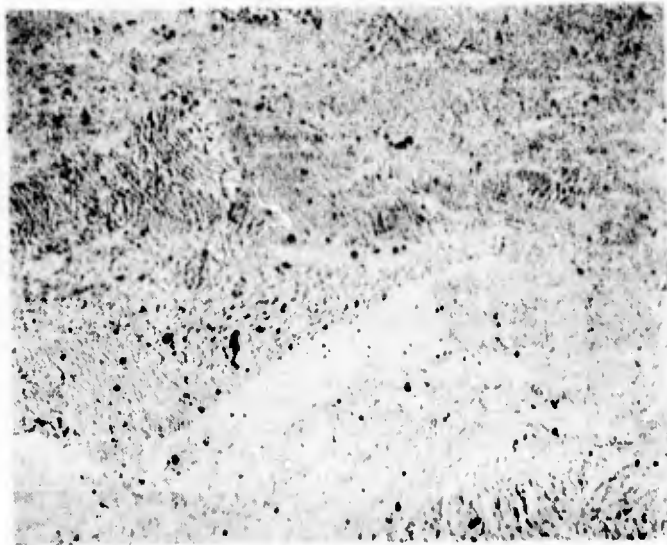Specimen R91, Mount H433 from plate
SA 27,030-BT.

FIGURE 39. - Worked β structure. (Originally 50X)
Specimen R-49, Mount G 275,
from plate SA 27,167-BB.

FIGURE 40. - Duplex structure of "defect" area.
            (Originally 6X)
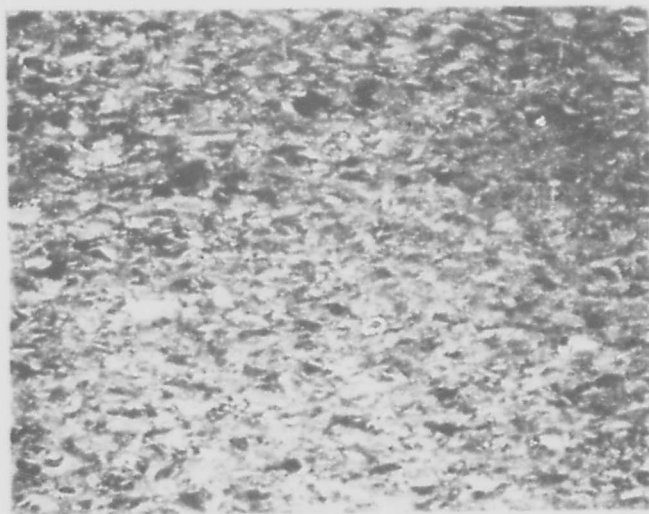   from plate SA 27,030-TB.

FIGURE 41. - Uniform structure of "defect-free" area.
(Originally 6X)
from plate SA 27,030-BB.

One example of a beta-rich stringer or band was found.
This was located in section BB of ingot SA 27,175. It
appears in the photomicrograph, Figure 42, as a dark etched
band with light etched grains dispersed in the dark etched
area. Microprobe analyses were made of the area and the
results are shown in Table XVIII. The dark, beta grains

TABLE XVIII. - Microprobe analyses of beta stringer

Structure	Al, %	V, %	N, %	O, %
Dark grains	4.2	6.5	<0.5	<0.5
Light grains	4.8	2.7	0.7	<0.5
Matrix	5.9	4.4	<0.5	<0.5

are rich in vanadium while the light alpha grains are low
in this element. Both phases have less than the normal
amount of aluminum. Nitrogen seems to reside mainly in
the bright-etched alpha-phase metal.

One major defect was indicated on the ultrasonic
chart for the triple-melt ingot SA 26,917, in the top (TT)
section. But metallographic examination did not reveal
any defect. The microstructure is shown in Figure 43 and
appears to be a normal alpha-beta structure with some areas
that have more than the normal amounts of alpha.

Figure 44 (also see Fig. 17) is a photomicrograph of
a defect area found in section TB of ingot SA 26,917, the
triple-melt ingot. This flaw was slightly less than one-
half inch long, and therefore it was not included in
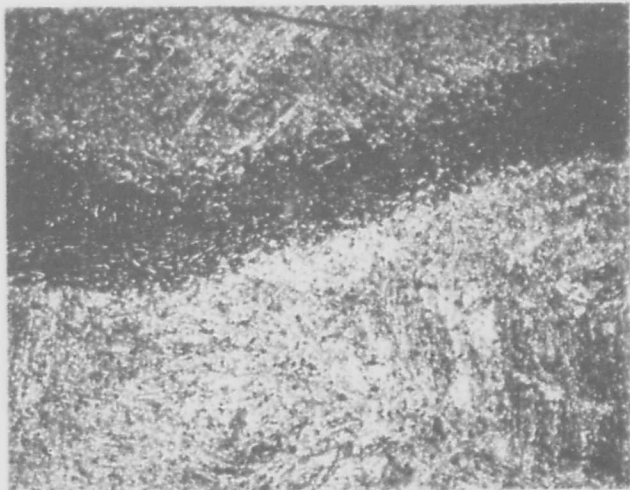Tables XV and XVI. It is a nitride-type defect which

84

FIGURE 42. - Beta-rich stringer (Originally 50X)
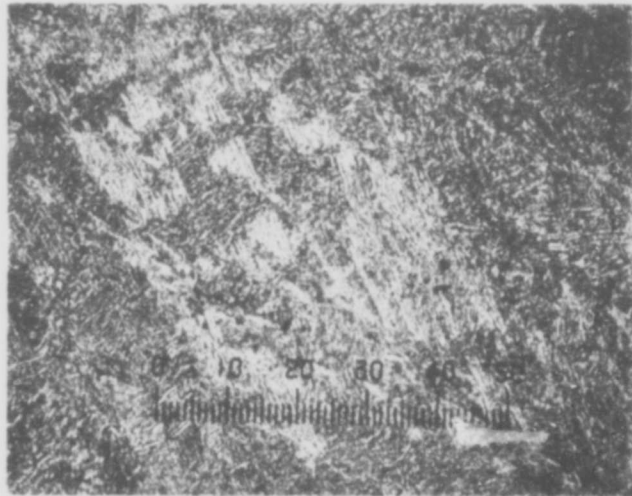   Specimen R-52, Mount G 308,
             from plate SA 27,175-BB.

FIGURE 43. - Excess α in α-β structure (Originally 50X)
Specimen R-45, Mount G 23,
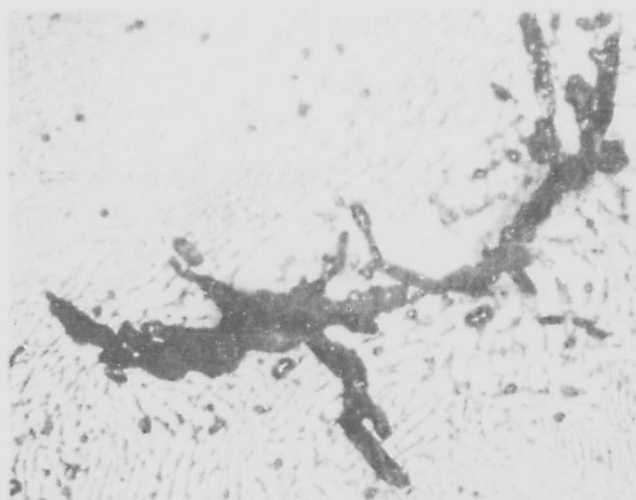from plate SA 26,917-TT.

FIGURE 44. - Nitride-type defect in triple-melt ingot.
(Originally 200X) Specimen R-37, Mount F 1288,
from plate SA 26,917-TB.

probably resulted from seeding of the sponge bars used for first-melt electrodes with Ti_xN. It differs in structure from nitride inclusions found in double-melt ingots in three ways. First, the nitrogen content is lower than usual; second, there appears to be branching of the defect area; third, the small voids around the main defect have the smooth, shiny appearance of gas holes. Microprobe analyses showed the flaw contained up to about 1.5% N. The alloy content was lower than in the matrix. The aluminum content was 5.4% and the vanadium, 2.1 to 2.5%. In the normal matrix material the aluminum was 6.3 and the vanadium 4.3%.

3.5 Discussion and Review

There is no doubt that nitride-induced defects survived in at least eight of the remelt ingots. Six of these were produced by the trial process based on first melting by skull casting into a side-gated mold. Therefore, the trial process has failed to eliminate the synthetic nitride inclusions. Nevertheless, evidence that some nitride was dissolved is contained in results of routine ingot analyses, the fact that nitride defects of Type II were formed (Figs. 15-17), and the diffusion of nitrogen from Type I inclusions into surrounding metal (Table XIV). But this still leaves some questions unanswered: How much nitride was dissolved? Was it enough to demonstrate any advantage for the trial process? Was it enough to indicate any merit in the general approach that might still be exploited? Were any other possible courses indicated?

Unfortunately, answers to the questions are clouded by inconsistencies among the attempts to evaluate the defectiveness of ingots. The most reliable technique is metallography, although it is possible to destroy or miss some small flaws in the course of taking specimens. But it simply is not practical to apply metallography broadly enough, and it is a technique that must be guided. That is, the site of a flaw must somehow be located before the

88

the presence of naturally occurring nitride in the sponge, but this is conjecture, of course, and other explanations are possible for this ingot. In any case, delta-phase nitrides of titanium are as much as half again as dense as titanium, so settling by gravity is possible. If a nitride lump reached the bottom of the molten pool without dissolving, it would probably be trapped there as an inclusion. The molten pools in CEVAR melting are very deep and typically extend well into the bottom halves of ingots.

Another factor that probably influenced the locations of flaws was nonuniform melting and solidification conditions. During the early part of a CEVAR cycle, the power input and metal superheat are low and freezing is relatively rapid due to proximity of the crucible bottom and the inherently higher surface-to-volume ratio of a short cylinder compared to a tall one. This situation surely was a major requisite to the formation of the Al-rich stringer and other nonnitride defects formed practically at the bottoms of ingots. It may also have contributed to the prevalence of nitride-induced flaws toward ingot bottoms. Regarding the Al-rich flaw, it may also be significant that it was found in an ingot for which part of the alloy addition was as elemental Al. Although only one nitride inclusion was discovered near the top of an ingot, the top parts of most ingots were rejected without examination for inclusions, and some were probably present. Presumably, these would have entered the molten pool late in the melting cycle when power was reduced for hot topping. Gravity would not have time to operate and chilling would not be highly efficient since the crucible bottom is far removed, and sidewall surfaces shrink away from the cooled copper as they solidify.

Despite the discovery of one nitride inclusion at the top of an ingot, and the probability that there were others, most of the bad features in the upper parts of ingots seemed to be unrelated to the nitride seeding. Carbon contamination, gasiness, grain boundary "dirtiness",

flaw can be examined metallographically. Neither ultrasonic inspection nor X-ray radiography ideally provides the requisite guidance. Ultrasound responds to all sufficiently discontinuous interfaces, including microstructural features as shown in Figures 19, 21, 37, 38, 39, and 40, and perhaps even more spurious things, whether they represent genuine flaws or not. In the investigation being reported here, it appears overall that most ultrasonic indications could not be metallographically verified as flaws. Ultrasonic inspection might be considered not selective enough, but radiography is too selective because the X-rays respond noticeably only to regions that are both sufficiently different than the matrix in X-ray transmittance and sufficiently thick compared to the thickness of the radiographic subject. Thus, for example, a gas bubble (or any other void) may not be detected if it is squeezed flat during a conversion operation. Yet this could represent a significant structural weakness. A good gauge of ingot quality with respect to alpha-stabilized voids and inclusions is still needed.

On the basis of this work, it would be quite difficult to choose between triple melting and double melting via skull casting. The triple-melt ingot, SA 26,917, and ingot SA 27,030 were similar metallographically, but ultrasonically SA 26,917 was among the cleanest ingots and SA 27,030 was the dirtiest. There was, however, another ingot, SA 27,167, that was ultrasonically similar to SA 26,917. Thus, it seems by either test that similar ingot quality can result from the two melting techniques. It is unlikely that the skull-melt-plus-remelt process is any better than triple melting, but without some information about the distribution of quality within a group of triple melts, it is not fair to suggest that triple melting is superior.

The tendencies for nitrogen in solution and nitrogen as nitride inclusions to be concentrated low in the ingots were probably related. Exhibition of the former tendency by the unseeded ingot, SA 27,172, could have resulted from

and difficulty in verifying ultrasonic flaw indications
were all greater for metal from the upper parts of ingots.
The extent of interrelation among these features is un-
known, but together with the nonnitride flaws low in
ingots, they seem to emphasize that nitride-induced de-
fects are far from the only problems of ingot quality.

Specific defects identified in this work were either
inclusions or segregated phase-stabilized regions. The
inclusions were either nitrogen-rich or carbon-rich, and
they could be distinguished visually by the presence of an
α-stabilized reaction zone around nitride inclusions and
the absence of such a zone around carbide inclusions. The
nitrogen-rich inclusions were more prevalent, undoubtedly
because most of them were artificially seeded. A strong
suspicion prevailed that some of the nitride inclusions
occurred naturally, but there was no way to verify this.
No two inclusions were quite the same, but nitride in-
clusions exhibited a wider range of characteristics than
the carbide inclusions did--probably because more of the
nitride inclusions were observed.

Segregated α- and β-stabilized regions each were ob-
served. Some of the α-stabilized regions clearly were
associated with localized nitrogen enrichment, but such
an association was not obvious in all cases. Neither was
such a convenient explanation available for the β-stabilized
region observed.

Besides the inclusions and segregates, ultrasonic
inspection indicated the presence of numerous apparent
defects that could not be confirmed specifically. Some
of these virtual flaws remain unexplained, but for others
two possibilities were identified, both likely related to
the thermomechanical conditions during metal conversion.
One irregularity was the formation of a coarse worked beta
or serrated alpha structure. The other was a layering of
duplex structures into a sandwich of coarse grains between
fine grains. The latter effect was more consistently
associable with the spurious defect indications.

4. CONCLUSIONS

The consumable-electrode vacuum arc remelting (CEVAR) of skull-cast first-melt ingots does not eliminate refractory nitride lumps. However, some dissolution of nitride does occur and the trial double-melting process seems capable of producing ingots of quality similar to a more conventional triple-melting procedure.

A nondestructive test or a combination of them that could somehow identify defects as well as locate them would be very useful. Spurious test responses also are troublesome and confusing.

Nitride-induced inclusions and voids are not the only serious defects of CEVAR ingots. Predisposing factors for forming any defect may include the properties of foreign materials or contaminants (especially refractoriness, solubility, and density) and irregularities of melting and solidification.

5. REFERENCES

1.   DeTemple, E., A. Gerhardt, and W. Knorr. Research
      on the Quality of Commercially Pure Titanium and
      Ti-6Al-4V Ingots. In The Science, Technology, and
      Application of Titanium, R.I. Jaffee and N.E.
      Promisel, eds., Pergamon Press, London, 1970, pp.
      35-41.

2.   Grala, E.M. Characterization of Alpha Segregation
      Defects in Ti-6Al-4V Alloy. Technical Report AFML-
      TR-68-304, TRW Inc. to Air Force Materials Lab (MAMP),
      Sept. 1968, 63 p.

3.   Grala, E.M. Effect of Melting on High Hardness
      Alpha Stabilized Areas in Ti-6Al-4V Alloy. Technical
      Report AFML-TR-71-65, TRW Inc. to Air Force Materials
      Lab (LL), May 1971, 36 p.

4.   Holmberg, B. Structural Studies on the Titanium-
      Nitrogen System. Acta Chemica Scandinavica, vol. 16,
      no. 5, 1962, pp. 1255-1261.

5.   Palty, A.E., H. Margolin, and J.P. Nielsen. Titanium-
      Nitrogen and Titanium-Boron Systems. Transactions
      of the ASM, vol. 46, 1954, pp. 312-328.

6.   Scanlan, J.V. and G.J.G. Chambers. Forgings in
      Titanium Alloys. In The Science, Technology, and
      Application of Titanium, R.I. Jaffee and N.E.
      Promisel, eds., Pergamon Press, London, 1970, pp.
      79-95.

7.   Wood, F.W. Elimination of Low-Density Inclusions
      in Titanium Alloy Ingots. Technical Report AFML-
      TR-69-47, Bureau of Mines to Air Force Materials
      Lab. (LTP), April 1969, 89 p.